A Comparison of New and Existing Equations for Estimating Sensible Heat Flux Density using Surface Renewal and Similarity Concepts

F. CASTELLVÍ[1], R.L. SNYDER[2], D.D. BALDOCCHI[3] and A. MARTÍNEZ-COB[(4)]

[1]University of Lleida, Spain

Corresponding address: Dpt. Medi Ambient i Cienciès del Sòl, E.T.S.E.A.Rovira Roure, 191, Lleida 25198. e-mail: f-Castellví@macs.udl.es

[2]University of California, Dept of Land, Air and Water Res, Davis, California, USA

[3]University of California, Dept of Environmental Science, Policy & Management, Berkeley, California, USA

[4]Dpto. Genética y Producción Vegetal, Est. Exp. Aula Dei (Consejo Superior de Investigaciones Científicas), Apartado 202, Zaragoza 50080, Spain.

KEYWORDS: Sensible heat flux density, Temperature standard deviation, Temperature structure function parameter, Temperature ramps.

ABSTRACT

This paper describes two approaches for estimating sensible heat flux, using surface renewal and similarity concepts. One approach depends on a temperature structure function parameter and is valid in the inertial sub-layer. The other approach depends on the temperature standard deviation and operates when measurements are made above the canopy top, either in the roughness or inertial sub-layer. The approaches were tested over turf grass, rangeland grass, wheat, grape vineyard and nectarine and olive orchards. It is shown that the free convection limit expression for the standard deviation method holds for slightly unstable conditions. When surface homogeneity and fetch requirements are not fully met in the field, the results show that the equations based on surface renewal principles are more robust and accurate than equations exclusively based on similarity backgrounds. It is likely that the two methods require no calibration unless the canopy is heterogeneous. Under unstable conditions, the free convection limit equation, which depends on the temperature

standard deviation, can provide on-line sensible heat flux density estimates using affordable battery-powered data logger with temperature data as the only input. The approach performed well when measuring near or well above the canopy top, thus, suggesting that the method is useful for long term monitoring over growing vegetation.

1. INTRODUCTION

Advances in methodology and instrumentation for measuring surface fluxes over natural surfaces have improved our understanding of soil-vegetation-atmosphere interactions. Selection of methods and instrumentation to determine surface fluxes depend on the accuracy required and the natural surface in question. Direct measurement is preferred, but not always is affordable. The use of precise lysimeters or the eddy covariance method for measuring latent and sensible heat flux is limited by the relatively high cost of both instruments and maintenance. It is, therefore, often desirable to obtain such estimates indirectly using low-cost and robust instrumentation. This explains the plethora of research on alternative methods such as flux-profile, Bowen ratio-energy balance, semi-empirical equations, etc. for estimating surface fluxes.

For estimating sensible heat flux, H, the surface renewal (SR) method [Higbie, 1935] in conjunction with the analysis of air temperature traces for estimating H over natural surfaces [Paw U et al.,1995] is attractive because it avoids many of the difficulties associated with similarity principles and it is less expensive. A summary of studies and applications on the SR analysis is provided in Katul et al [1996], Castellví [2004] and Paw U et al. [2005]. Similarity relationships are valid in the constant flux layer over the surface, well above the zero-plane displacement and roughness length for momentum, so fetch requirements and difficulties in sensor access due to canopy height are important. The SR analysis is applicable close to the surface and, because of lower cost, replication to achieve good spatial coverage is easier than with more costly methods. For water management, SR analysis for estimating H is attractive because, through a surface energy-balance closure, latent heat flux, or crop water use rates, can be estimated as the residual of the energy balance equation [Anderson et al., 2003].

In SR analysis, air temperature data are measured at high frequency and most battery-powered data-loggers are still too slow to record and process data simultaneously for providing H estimates. In SR analysis, calibration to account for unequal heating below the sensor height is required, and the calibration coefficient changes as the vegetation grows [Castellvi, 2004]. Our purpose was to automatically account for calibration coefficient changes, to keep instrumentation simple, inexpensive and accessible, and to avoid

problems associated with large datasets. Two new approaches for estimating H using SR analysis were derived assuming ideal field conditions (i.e., a flat, extensive and homogeneous surface); however, such conditions are frequently not met in field trials. Therefore, method performance was also tested over heterogeneous canopies. One of these two new approaches, which depends on the standard deviation and the third order structure function of the temperature, produced reliable results from data recorded in either the inertial or roughness sub-layers and it was simple enough to allow on-line data-logger calculation of H under unstable atmospheric conditions.

2. METHODS

2.1 Theory and short background

During the last decade, SR analysis appeared as an attractive method for estimating sensible heat flux. Several studies have analysed the SR method and improved understanding of earlier models [Gao et al., 1989; Paw. U et al., 1992 and 1995; Qiu et al., 1995; Katul et al., 1996; Snyder et al., 1996; Chen et al., 1997a and 1997b; Spano et al., 1997 and 2000; Zapata and Martínez-Cob, 2001; Castellví et al., 2002; Castellví, 2004; Castellví and Martínez-Cob, 2005; and Paw U et al., 2005]. SR analysis assumes that turbulent exchange, on any scalar is driven by the regular replacement of the air parcel in contact with the surface where exchange occurs. As one air parcel sweeps down to the surface, it replaces another that is ejected from the canopy, once the latter has enriched or depleted the scalar. SR models are based on the fact that most of the turbulent transfer is associated with large-scale coherent eddies, which are evident as scalar ramp-time series. An ideal and comprehensive scheme for this process was originally presented by Paw U et al. [1995] and Chen et al. [1997a]. Sensible heat flux from the surface at height, z (within the canopy, in the roughness or inertial sub-layer), over the averaging period (commonly half-hour) is determined by the following expression [see among others, Paw U et al. 1995; Snyder et al., 1996 and Chen et al., 1997a]

$$H = (\alpha z)\, \rho C_p \frac{A}{\tau} \qquad (1)$$

To shorten the paper, the definitions of symbols is provided in the glossary. A practical method for estimating ramp dimensions according to ramp model shown in Figure A.1 [Chen et al.,1997a] is presented in Appendix A. The variable (αz) is the volume of air, with height z per unit ground area, exchanged on average for each ramp in the sample period. The variable (αz) was also interpreted as the mean eddy size responsible for the renewal process that fits the local air temperature gradient. The following relationship was proposed when measuring above the canopy [Castellví, 2004]

$$\frac{A}{(\alpha\, z)} \propto \frac{dT}{dz} = \begin{cases} \beta \dfrac{A}{(z - d)} & z > z^* \\ \beta \dfrac{A}{z} & h \le z \le z^* \end{cases} \qquad (2)$$

The parameter β may be interpreted as a dimensionless aerodynamic resistance of the number of ramps formed during a given period, and z* is the roughness sub-layer depth. In (2) the eddy size was scaled as, (z - d) and z, when measuring well above and close to the canopy, respectively [Kaimal and Finnigan, 1994; Chen et al., 1997b]. Following Castellvi [2004], parameters α and β are estimated as,

$$\alpha = \begin{cases} \left[\dfrac{k}{\pi} \dfrac{(z-d)}{z^2} \dfrac{\tau u_*}{\phi_h(\varsigma)} \right]^{1/2} & z > z^* \\ \left[\dfrac{k}{\pi} \dfrac{z^*}{z^2} \dfrac{\tau u_*}{\phi_h(\varsigma)} \right]^{1/2} & h \le z \le z^* \end{cases} \qquad (3)$$

$$\alpha \beta = \begin{cases} \dfrac{(z-d)}{z\pi} & z > z^* \\ \dfrac{1}{\pi} & h \le z \le z^* \end{cases} \qquad (4)$$

Combining Eqs.(1), (3) and (A5) from the appendix A with the Obukhov length, L_o, gives the equation

$$L_o = \frac{u_*^3}{\left(\dfrac{k\,g}{\rho}\right)\left(\dfrac{H}{T C_p} + 0.61E\right)} \approx -\rho C_p \frac{u_*^3}{\left(\dfrac{k\,g}{T}\right) H} \qquad (5)$$

where the right-hand expression is traditionally used for dry climates. Castellví [2004] proposed estimating sensible heat flux as

$$H = \begin{cases} \rho C_p \left(\dfrac{g}{T}\right)^{1/5} \dfrac{\left(k(z-d)\right)^{4/5}}{\pi^{3/5}} \left(-\gamma^3 \dfrac{S^3_{(rx)}}{r_x}\right)^{3/5} A^{-3/5} \left(\dfrac{\phi_h^{-3}(\varsigma)}{-\varsigma}\right)^{1/5} & z > z^* \\ \rho C_p \left(\dfrac{g}{T}\right)^{1/5} k^{4/5} \left(\dfrac{z^*}{\pi}\right)^{3/5} z^{1/5} \left(-\gamma^3 \dfrac{S^3_{(rx)}}{r_x}\right)^{3/5} A^{-3/5} \left(\dfrac{\phi_h^{-3}(\varsigma)}{-\varsigma}\right)^{1/5} & h \le z \le z^* \end{cases} \qquad (6)$$

2.2 Method description

Combining Eqs. (1), (5) and (A5), the friction velocity for dry climates can be expressed as

$$u_* = \begin{cases} \left[\alpha \gamma^3 (z-d) z \dfrac{kg}{T A^2} \left(\dfrac{S^3_{(r_x)}}{r_x} \right) \right]^{1/3} \dfrac{1}{\varsigma^{1/3}} & z > z^* \\ \left[\alpha \gamma^3 z^2 \dfrac{kg}{T A^2} \left(\dfrac{S^3_{(r_x)}}{r_x} \right) \right]^{1/3} \dfrac{1}{\varsigma^{1/3}} & h \le z \le z^* \end{cases} \tag{7}$$

Combining Eqs.(3) and (7), friction velocity can be rewritten as

$$u_* = \begin{cases} \left[\left(\dfrac{g}{T} \right)^2 \left(k (z-d) \right)^3 \dfrac{\gamma^3}{\pi} A^{-1} \left(-\dfrac{S^3_{(r_x)}}{r_x} \right) \right]^{1/5} \left(\varsigma^2 \phi_h(\varsigma) \right)^{-1/5} & z > z^* \\ \left[\left(\dfrac{g}{T} \right)^2 \left(k^3 z^2 z^* \right) \dfrac{\gamma^3}{\pi} A^{-1} \left(-\dfrac{S^3_{(r_x)}}{r_x} \right) \right]^{1/5} \left(\varsigma^2 \phi_h(\varsigma) \right)^{-1/5} & h \le z \le z^* \end{cases} \tag{8}$$

Equation (8) is consistent with the parameters needed to describe turbulence under convective conditions, as turbulence becomes independent from the stability parameter and friction velocity. The function $(\zeta^2 \phi_h(\zeta))^{-1/5}$ can be approximated to a constant with a value of 1.2 that produces relative errors of less than 10% for $\zeta \le -1$. For free convection, according to Högström [1990], Eq. (8) tends to be decoupled from the surface since the ramp dimensions are greatly influenced by the boundary layer scale eddies. Under near neutral conditions, both ζ and $S^3_{(r)}$ tend to 0, giving a finite value.

2.2.1. Measuring well above the canopy in the inertial sub-layer. Assuming ideal field conditions, Monin-Obukhov similarity theory holds for measurements in the inertial sub-layer and it is known that

$$\frac{(z-d)}{T_*} \frac{dT}{dz} = k^{-1} \phi_h(\zeta) \tag{9}$$

Using Eqs. (2) and (9), an expression that combines surface renewal with similarity concepts is

$$\frac{A}{T_*} = (k \beta)^{-1} \phi_h(\zeta) \tag{10}$$

Two well established similarity-relationships ($g_1(\zeta)$ and $g_2(\zeta)$), which also involve T_*, were originally given in Wyngaard et al. [1971], Eq. (11), and Tillman [1972], Eq. (12),

$$\frac{C_{tt}}{T_*^2} = (z-d)^{-2/3} g_1(\varsigma) \tag{11}$$

$$\frac{\sigma_T}{T_*} = g_2(\varsigma) \tag{12}$$

Equations (10), (11), (12), and (7) are used to express the sensible heat flux density ($H=\rho C_p T_* u_*$.) in two different forms:

(1) When the temperature structure function parameter, C_{tt}, is known:

$$H = \rho C_p \left[\gamma^3 (z-d)^{4/3} \frac{kgz}{T} C_{tt}^{1/2} \left(-\frac{S_{r_x}^3}{r_x} \right) \right]^{1/3} \left(\alpha\, (k\beta)^2 \frac{\phi_h^{-2}(\varsigma) g_1^{-1/2}(\varsigma)}{-\varsigma} \right)^{1/3} \tag{13}$$

(2) When the temperature standard deviation, σ_T, is known:

$$H = \rho C_p \left[\gamma^3 (z-d) \frac{kgz}{T} \sigma_T \left(-\frac{S_{r_x}^3}{r_x} \right) \right]^{1/3} \left(\alpha\, (k\beta)^2 \frac{\phi_h^{-2}(\varsigma) g_2^{-1}(\varsigma)}{-\varsigma} \right)^{1/3} \tag{14}$$

2.2.2. Measuring above the canopy in the roughness sub-layer. Within the roughness sub-layer, similarity-based relationships may be invalid. Based on flux-gradient relationships, for homogeneous canopies - according to Cellier and Brunet [1992] - sensible heat flux can be estimated using the expression, $H=\rho C_p K^*_h dT/dz$, with K^*_h the eddy diffusivity for heat in the roughness sub-layer. Denoting $\phi_h^*(\zeta)$ as an appropriate stability function for heat in the roughness sub-layer, Cellier and Brunet [1992] found the following relationship: $\phi_h^*(\zeta)/\phi_h(\zeta)= K_h/K^*_h \sim (z-d)/z^*$. Since $K_h=ku_*(z-d)\phi_h^{-1}(\zeta)$ is a suitable expression for the eddy diffusivity for heat in the inertial sub-layer [Brutsaert, 1982], it follows that the eddy diffusivity for heat in the roughness sub-layer can be estimated as,

$$K_h^* = k u_* z^* \phi_h^{-1}(\zeta) \tag{15}$$

Assuming that the ratio of similarity-relationships in Eqs. (10) and (12), $\phi_h(\zeta)/g_2(\zeta)$, also holds true in the roughness sub-layer through a given proportionality, μ, as

$$\frac{(k\beta)A}{\sigma_T} = \left(\phi_h(\varsigma) \big/ g_2(\varsigma) \right) = \mu \left(\phi_h^*(\varsigma) \big/ g_2^*(\varsigma) \right) \qquad (16)$$

where $g^*_2(\zeta)$ denotes the corresponding $g_2(\zeta)$ valid in the roughness sub-layer. Experimentally, the assumption made in the second equality of equation (16) is supported by the literature. Lloyd et al.[1991] that found that the form of $g_2(\zeta)$ is independent of the terrain type; Hsieh et al.[1996] and Wesson et al. [2001] found that $g_2^*(\zeta)$ for non-uniform surfaces is proportional to $g_2(\zeta)$. Cellier and Brunet [1992] and Hsieh et al.[1996] found that the form of $\phi_h(\zeta)$ is rather robust to non-uniform ground heating condition. Combining Eqs. (2), (7), (15), (16) and $H=\rho C_p K^*_h dT/dz$ therefore gives the following expression for estimating the sensible heat flux in the roughness sub-layer is obtained

$$H = \rho C_p \left[\frac{(\gamma z^*)^3}{z} \frac{kg}{T} \sigma_T \left(-\frac{S^3_{r_x}}{r_x} \right) \right]^{1/3} \left(\alpha\,(k\beta)^2 \frac{\phi_h^{-2}(\varsigma) g_2^{-1}(\varsigma)}{-\varsigma} \right)^{1/3} \qquad h \le z \le z^* \qquad (17)$$

where the parameter μ ,in Eq. 16, was set equal to 1.0 for practical application. Equation (16) was obtained after equating T_* from equations (10) and (12), so it was expected that the portion μ be a constant close to the unity. The dependence in equation (17) on parameter μ is through the power 1/3. Then, if μ slightly departs from 1.0, the total error introduced in H is diminished.

The dependence of Eqs.(13), (14) and (17) on the stability parameter requires experimental evidence. Consequently, previous knowledge of the measurement methods is required. In Appendix B, it is shown that: (1) under slightly unstable conditions, the three equations permit estimation of H from air temperature measurements, (2) under moderately stable conditions, wind speed measurement is also required, and (3) under strong stability conditions, the equations appear to be only dependent on temperature measurements although similarity is uncertain under such conditions.
Appendix B shows that, under unstable conditions, the different expressions permit H estimation as follows.

When the temperature structure function parameter is known,

$$H = \rho C_p \left(1.65\, \gamma \frac{k^{5/6} g^{1/3}}{\pi^{1/2}} \right) (z - d)^{7/9} \left[\frac{C_{tt}^{1/2}}{T} \left(- \frac{S_{r_x}^3}{r_x} \right) \right]^{1/3} \qquad z \geq z^* \qquad (18)$$

When the temperature standard deviation is known,

$$H = \begin{cases} \rho C_p \left(1.65\, \gamma \frac{k^{5/6} g^{1/3}}{\pi^{1/2}} \right) (z - d)^{2/3} \left[\frac{\sigma_T}{T} \left(- \frac{S_{r_x}^3}{r_x} \right) \right]^{1/3} & z \geq z^* \\ \rho C_p \left(1.65\, \gamma \frac{k^{5/6} g^{1/3}}{\pi^{1/2}} \right) z^{1/6} \left(z^* \right)^{1/2} \left[\frac{\sigma_T}{T} \left(- \frac{S_{r_x}^3}{r_x} \right) \right]^{1/3} & h \leq z \leq z^* \end{cases} \qquad (19)$$

Equations (18) and (19) express the free convection limit approaches for Eqs. (13), (14) and (17), respectively. According to Appendix B the free convection limit is reached for $\zeta \leq -0.1$, though it likely may hold for a wider range. This requires experimental evidence. The free convection limit for Eq.(6) holds in the interval, $-3 \leq \zeta \leq -0.03$, with a relative error of less than 8.5% [Castellvi, 2004]. Therefore, when the ramp amplitude is known, the sensible heat flux can be estimated as

$$H = \begin{cases} \rho C_p \left(2.4 \gamma^{9/5} \frac{k^{4/5} g^{1/5}}{\pi^{3/5}} \right) \left[\frac{(z-d)^4}{T} \right]^{1/5} \left(- \frac{S_{(rx)}^3}{r_x} \right)^{3/5} A^{-3/5} & z > z^* \\ \rho C_p \left(2.4 \gamma^{9/5} \frac{k^{4/5} g^{1/5}}{\pi^{3/5}} \right) \left[z \frac{(z^*)^3}{T} \right]^{1/5} \left(- \frac{S_{(rx)}^3}{r_x} \right)^{3/5} A^{-3/5} & h \leq z \leq z^* \end{cases} \qquad (20)$$

Equations (18), (19) and (20) express sensible heat flux in W m^{-2} when all the input variables are given in SI units. For applying Equations (18), (19) and (20), previous knowledge of the atmospheric stability condition of the surface layer during each sample is required. The sign of the third moment of the temperature structure function coincides with the sign of the stability parameter, see (A5) [Van Atta, 1977; Antonia et al., 1981].

2.3 Existing similarity-based equations for estimating sensible heat flux

The main objective was to analyse the performance of the new approaches presented for estimating sensible heat flux. It is interesting, however, to examine the performance of several other equations from the literature; especially those requiring the same measurements or input parameters. Thus, we analysed the similarity-based expressions originally presented by Wyngaard et al. [1971] and Tillman [1972] for estimating sensible heat flux that respectively involve the temperature structure function parameter, Eq. (21), and the temperature standard deviation, Eq. (22).

$$H = \rho C_p \left(\frac{kg}{T} \right)^{1/2} (z-d) \left(\frac{(g_1(\varsigma))^{-3/2}}{-\varsigma} \right)^{1/2} (C_{tt})^{3/4} \qquad z > z^* \tag{21}$$

$$H = \rho C_p \left(\frac{kg\,(z-d)}{T} \right)^{1/2} \left(\frac{(g_2(\varsigma))^{-3}}{-\varsigma} \right)^{1/2} (\sigma_T)^{3/2} \qquad z > z^* \tag{22}$$

The respective free convection limit approach, for the two equations, is as follows

$$H = \rho C_p \left(0.8 (kg)^{1/2} \right) \frac{(z-d)}{T^{1/2}} (C_{tt})^{3/4} \qquad \varsigma << -0.14 \tag{23}$$

$$H = \rho C_p \left(1.08 (kg)^{1/2} \right) \left(\frac{(z-d)}{T} \right)^{1/2} (\sigma_T)^{3/2} \qquad \varsigma < -0.04 \tag{24}$$

These last four equations (mainly the flux-variance method, Eqs. (22) and (24)), have been the subject of intensive research [Wesely, 1988; Weaver, 1990; Kader and Yaglom, 1990; Lloyd et al., 1991; Padro, 1993; De Bruin et al., 1993; Alberston et al., 1995, Katul et al., 1995 and 1996; Hsieh and Katul, 1996; Wesson et al., 2001; and Castellví and Martínez-Cob, 2005]. Similarity theory holds over an extensive, flat and homogeneous terrain. Such conditions, however, are often difficult to find and; therefore, the performance of similarity theory under non-ideal conditions is of interest. The flux-variance method, commonly used by many micrometeorologists, has been analysed under different field conditions including non-uniform terrain, advective conditions and close to the canopy [Weaver, 1990; De Bruin et al., 1991; Katul et al., 1995; Wesson et al., 2001]. These analyses could be useful for different purposes. Methods providing evapotranspiration errors below 25%, for irrigation planning, and methods for estimating surface fluxes providing a deficit closure of the energy budget up to 30%, for model calibration, may be still feasible [Twine et al., 2000; and Kustas et al., 1999].

2.4 Advantages, limitations, minimum instrumentation, and data processing requirements.

2.4.1 *Advantages and limitations for field applications*. Equations (6), (13), (14), (21) and (22) operate when measurements are made well above the canopy top. Equations (6) and (17) operate close to the canopy top and; therefore, are useful when fetch and accessibility to sensors are a limitation. All these six equations are comparable in terms of input data. The term, $\rho C_p \approx 1215$ J m^{-3} K^{-1}, for a wide range of climates, therefore, they require wind speed and high frequency air temperature measurements. However, their respective free convection limit approaches are not comparable. Unless other techniques, based on the scintillation theory, are available for determining the temperature structure function parameter in Equations (18) and (23), a minimum of two thermocouples or a thermocouple and a cup anemometer in conjunction with the Taylor hypothesis of frozen turbulence is required for field measurements. The other free convection limit approaches, using Eqs. (19), (20) and (24), require a single thermocouple.

Equations (19) and (24) are directly comparable. Because previous knowledge of the surface layer atmospheric stability is required, if a third order temperature structure function is used to identify unstable conditions, then the same calculations are needed for Eqs. (19) and (24). Other methods to identify unstable atmospheric conditions may be used. For example, Wesson et al. [2001] assumed unstable conditions when net radiation was positive, but this involves extra measurements and maintenance. We note that we may often have positive net radiation and stable conditions during afternoon in arid environments. Recall that Eq.(24) does not necessarily hold when measurements are made close to the canopy top.

Equations (6), (13), (14), (17), (21) and (22) need to be solved on a computer because they depend on the stability parameter. Sensible heat flux from Eq. (20) cannot be recorded on-line using slow battery-powered data loggers. The ramp amplitude computation is needed, and data logger speed limits processing of the high frequency temperature data.

Overall, depending on the required accuracy, Eq. (19) is likely adequate under unstable conditions. A single thermocouple is required and measurements can be taken close to or well above the canopy top.

2.4.2 *Minimum instrumentation and data processing requirements.* Low-budget measurement campaigns require minimization of maintenance, inexpensive and robust instrumentation, and, if possible, on-line estimation of H to minimize visits to the site. Equations (19) and (24) require the minimum logger and sensor requirements for estimating H under unstable conditions; a fine-wire thermocouple and a data-logger. Thermocouples with smaller diameter are more responsive and more accurate, but thermocouples with larger diameter are less prone to damage. In Duce et al. [1998] is shown that half-hourly structure functions determined with different diameter wire size affected the ramp parameters determination. Thermocouples like the TCBR-3 ($7.6\ 10^{-5}$ m diameter) permit high frequency (4 or 8 Hz) measurements and they are infrequently damaged by rainfall and other hazard events. Smaller thermocouples need more frequent replacement. A data-logger capable of storing half-hourly temperature standard deviations and the third order structure function for several time-lags is required. Generally, three time lags is sufficient if a reasonable estimate of rx is available (see Table A.1). The sampling frequency requirement is limited mainly by the processing time needed between samples. The appropriate sampling frequency depends on the canopy size and how close to the canopy top measurements are taken. For example, tall and dense forest canopies could be monitored using a frequency of about 4 Hz. For moderate tall, sparse or dense canopies (e.g., nectarine or olive orchard as described next), near canopy top measurements with time-lags of about 0.5 s and 4 Hz measuring frequency may be adequate. For shorter canopies (e.g., grasses, wheat, etc.), it is better to measure 0.5 to 1.0 m above the canopy top [Snyder et al., 1996]. Appropriate time-lags are about 0.2 s, therefore, sampling frequencies of 8 Hz are suitable [Castellvi, 2004]. Under windy conditions, higher frequency measurements might be needed because of the high absorption of momentum. During near neutral and stable conditions, ramps are often not in agreement with the sign of the measured H; however, it is a minor problem because the H values are typically low. Therefore, measurement frequencies greater than 4-8 Hz are unnecessary for most field applications under unstable conditions. A data-logger such as a Campbell Scientific, Inc. CR10X meets the requirements to collect the standard deviation and 3^{rd} moment for several time lags.

With this datalogger, computation of temperature differences for three different time lags in order to obtain three half-hour structure functions requires an execution time of 0.136 s. Then, the minimum possible time execution interval to be implemented in a CR10X would be 0.15625 s (6.4 Hz), and three half-hour structure functions, corresponding to time lags of 0.15625 s, 0.46875 s and 0.625 s, could be computed and stored in datalogger memory, allowing on-line H calculation. On-line computation of latent heat flux through a simplified surface energy-balance [Allen et al., 1996] could also be implemented when additional instrumentation for measuring half-hour net radiation, wind speed and direction, and soil heat flux (using two soil heat flux plates and a soil-averaging temperature sensor), is also connected to the same CR10X datalogger. However, in some instances, storing these other parameters on-line can lead to small errors due to inadequate data logger computational speed. Generally, such errors will have minimal effect on the H estimate or LE estimates. Using a CR10X, an execution time interval of 6.4 Hz would not be enough for accomplishing all computation steps required: every half-hour, between 1 and 7 % of the temperature differences calculated for structure function computation would be missed or not accurately computed, depending on time-lag considered. These errors in H calculation would be small in general, however, to avoid such situations the alternatives are: 1) use of two CR10X dataloggers, one for on-line H computation and the other for recording the other variables required for the energy balance closure; 2) use of a single CR10X datalogger with a higher time execution interval, for instance, 0.25 s (4 Hz); or 3) use of somewhat more powerful datalogger such as the CR23X (CSI) as its cost is less than that of two CR10X and its processing speed is significantly higher.

2.5 Site description, instrumentation, and data

The data set used to analyse the performance of different equations for estimating sensible heat flux corresponds to several measurement campaigns conducted over distinct surfaces and climates. A summary of the main characteristics of the campaigns is given in Table 1. Six different canopies were analysed: grass closely meeting the reference crop definition [Allen et al., 1998], wheat, grapevines, rangeland grass and nectarine and olive orchards. Details about the campaigns conducted over grass, wheat and grapevines and data processing can be found in Snyder et al.[1996], Spano et al.[1997 and 2000] and Castellví [2004], and for the olive orchard in Castellví and Martínez-Cob [2005].

A brief overview is as follows. Three experiments over grass (0.1 m high) were carried out at same experimental site during different years. Instrumentation was set at the middle of a 100 m x 100 m plot at the Campbell Tract Experimental Farm (University of California at Davis). Half-hourly mean wind speed at 2 m above the ground was available. A omni dimensional sonic anemometer (Csi), measuring vertical wind speed and air temperature at 10 Hz, was set at 0.6 m above the ground level during days of year 86, 87 and 88 in 1994 and at 0.7 m during days of year 213 and 214 in 1995. Air temperature data at 8 Hz was also recorded at heights of 0.6, 0.9 and 1.2 m in year 1994, and at 0.7, 1.0 and 1.3 m in year 1995 using fine-wire thermocouples (7.6 10^{-5} m diameter). For these two campaigns, measurements were taken under unstable conditions. A three dimensional sonic anemometer (Csi), measuring three wind components and air temperature at 10 Hz, was set at 1.5 m from days 222 to 234 in 2001. Fetch requirement for the grass experiments was short (50 to 60 m) according to the rule of thumb, 1:100 (a fetch of 100 m is needed to account for one meter adjusted boundary layer depth), Stull (1991). This rule is useful for practical purposes though recognized rather conservative (Monteith and Unsworth, 1990). The grass plot was surrounded by short irrigated crops in the main upwind direction and bare soil. Because the surface roughness, within several hundred meters, was similar, it is realistic to assume that the wind profile was not disturbed by the transition. For the experiment conducted in year 2001, the averaged half-hourly wind speed at 1.5 m height, friction velocity, and stability parameter were, respectively; 1.9 m s^{-1}, 0.13 m s^{-1} and –0.91, under unstable conditions and 2.0 m s^{-1}, 0.14 m s^{-1} and 0.43 for the stable cases. For the other experiments, the averaged half-hourly horizontal wind speed at 2.0 m height, friction velocity and stability parameter were, respectively; 2.4 m s^{-1}, 0.20 m s^{-1} and –0.05 for year 1994, and 1.6 m s^{-1}, 0.13 m s^{-1} and –0.08 for year 1995. Foot print analysis was carried out according to Kormann and Meixner (2001). The cumulative mean upwind foot print determined under unstable conditions was: 89 % for year 2001 at 1.5 m, 81% for 1994 at 1.2 m, and 0.80% for 1995 at 1.3 m. However, under stable conditions only 36 % was accounted at 1.5 m. Therefore, whatever the level and experiment, most of measurements were rather representative for the grass plot under unstable conditions. But some contamination in the traces by the surroundings is expected under stable conditions.

The wheat experiment (0.7 m high) was conducted during days of year 148 and 149 in 1994 at Davis (Ca). Fetch was over 400 m. Half-hourly wind speed was measured at 2 m above the ground, air temperature at 8 Hz was measured at 0.7, 1.0 and 1.3 m above the ground using fine-wire thermocouples (7.6 10^{-5} m diameter) and an omni dimensional sonic anemometer (Csi) was set at 2 m above the ground measuring the vertical wind speed and air temperature at 10 Hz.

The experiment conducted over grapevines having 2.0 m height, 60% ground cover and separation between trunks of 1.5 m between plants and 2.7 m in the inter-row with a mean free space of 1.8 m. The experiment was conducted during days of year 226 and 227 in 1995 at Napa Valley (Ca). Fetch was over 300 m. Half-hourly wind speed was measured at 3 m above the ground, air temperature at 8 Hz was measured at 2.0, 2.3, 2.6 and 2.9 m above the ground using fine-wire thermocouples (7.6 10^{-5} m diameter), and an omni dimensional sonic anemometer (Csi) was set at 3 m above the ground measuring the high frequency vertical wind speed and air temperature at 10 Hz.

The experiment conducted over olive orchard (3.4 m high, 50% ground cover, 3 m separation between trunks with an inter-row of 6 m wide) occurred in days of year 106 to 208 in 1995 at Sástago within the Ebro river basin (NE of Spain). Fetch was about 550 m for the mean stream-wind direction (north-west). Air temperature at 4 Hz was measured at 3.5 and 5.1 m above the ground using fine-wire thermocouples (7.6 10^{-5} m diameter) and a three dimensional sonic anemometer (Csi) was set at 4.9 m above the ground measuring the three wind speed components and air temperature at 10 Hz. The temperature structure functions of order 2, 3 and 5, Eq.(A1), were recorded in a data-logger (CR10X) at two time lags, 0.25 s and 0.75 s.

The rangeland grass experiment, with 0.25 m for the mean vegetation height, is fully described in Baldocchi et al. [2004]. Briefly, the site is a grazed grassland opening in a region of oak/grass woodland. The site is situated in undulating topography among the oak/grass savannah biome of eastern California in the foothills of the Sierra Nevada Mountains. The main grass and herb species include bromus, frescue, oat, medusa head and rose clover. The site is dry and warm during mid spring, summer and early fall. Regional advection is a typical climate feature during summer and early fall. Often, the atmospheric surface layer tends to near neutral atmospheric stability conditions at around 1900 h (GMT) in spring and 1600 h (GMT) in summer and fall, and stability persists until sunrise. The sensible heat flux ranged from -78 to 473 W m^{-2}. A three-dimensional sonic anemometer (Gill Windmaster Pro) was installed at a height of 2 m. Virtual temperature and three wind components were recorded at 10 Hz over mid-spring through early fall in 2002.

The nectarine orchard experiment was conducted in summer 1989 (Atalia, Portugal). The average tree height was 3.2 m, the ground cover was approximately 85% and separation between trunks was; 3.5 m between trees and 5 m in the inter-row with a mean free space of 1.5 m. A thermocouple (7.6 10^{-5} m diameter) was located between trees at the canopy top height and measuring air temperature at 8 Hz. The variance and covariance of vertical wind speed and temperature were measured using a omni dimensional sonic anemometer (Csi) that was set at 3.5 m height, recording processed half-hourly H values from raw data at 10 Hz.

2.6 Canopy parameters

Equations for estimating H may operate close or well above the canopy top. Therefore, knowledge of z^* is crucial for placing sensors, but this requires the analysis of the wind and temperature profiles. Because the aim is to keep low-budget experiments, the roughness layer depth needs to be estimated. Roughly, this may be possible because z^* is highly dependent on the canopy morphology and its capability on absorbing momentum. Such dependence may be described through the canopy height, h, the mean spacing of roughness elements, D, and the zero plane displacement which in turn is also highly dependent on the canopy morphology.

2.6.1 *The zero plane displacement*. It can be estimated as, $d \approx 2/3h$ [Brutsaert, 1982] for the homogeneous canopies (grass, rangeland grass and wheat). For grapevines and nectarine orchard it was also roughly estimated as 2/3 h because in the mean stream-wise direction the canopy was dense and overlap through close to the ground and the mean inter-row space was moderate (1.8 m and 1.5 m, for grapevines and nectarines, respectively). For the olive orchard, the zero plane displacement was neglected because the canopy was open without understories and the crown was not dense [Brutsaert, 1982]

2.6.2 *The roughness sub-layer depth*. For tall and rather homogeneous canopies, such as forest, the roughness sub-layer depth is estimated to be about 2 and 3 times h [Kaimal and Finnigan, 1994; Shaw, 2002]. In general, Brutsaert [1982] reports a wider range; from 1.5 to 3.5 times the canopy height and some studies used the following approach, $z^* \approx h+2(h-d)$ [Chen et al., 1997a; Sellers et al., 1986] which falls in a lower range. For sparse tall canopies, z^* can be estimated as, $z^* \approx aD + d$ [Garrat, 1980], where D is the mean spacing of roughness elements and $a \approx 3$ is a coefficient. Higher values for a often occur under near-neutral stability conditions ($a = 4.6$, at neutral conditions). For crops, Cellier [1986] suggested $z^* \approx aD + d$ with D the inter-row space for canopies planted in rows and *a,* a coefficient likely slightly higher than 3. Cellier and Brunet [1992] reported $a = 3.1$ for sugar cane crop and $a = 4.2$ for maize.

Over grass and rangeland grass, measurements lie well above the roughness sub-layer. Therefore, z^* was only estimated for the other canopies. For wheat, because the canopy was uniform and measurements were made under unstable conditions with moderate wind speeds (mostly lower than 2.5 m s^{-1} at z = 2 m) z^* was estimated as $z^* \approx h+2(h-d) \approx 1.2$ m. The highest measurement level was at 1.3 m which is close to the transition roughness-inertial sub-layer. For the other measurement levels, the data were most likely collected within the roughness sub-layer.

For grapevines, the roughness depth was assumed to be, z^*=5.5 m, which is in between three times the mean space between canopies along the inter-row and three times the canopy height.

For the nectarine orchard, because the canopy extent was rather dense, z^* was estimated as, z^* = 9.5 m (about 3 times the canopy height). The roughness depth estimated as three to four times the mean inter-row canopy space results z^* to be in the range, $4.5 \leq z^* \leq 7.5$ m. The latter appears rather close to the canopy top and too short than for the rule of about three times the canopy height.

For the olives orchard, the coefficient *a* = 3.5 was used as an intermediate value between 3 and 4, which was chosen because the area is windy and therefore turbulence is mostly mechanically driven. Then, the roughness depth was estimated as, $z^* \approx 12$ m, which is about 3.5 times the distance between trunks (3.5 m). The mean spacing between canopies was taken as 3.5 m because the canopy was not dense. The estimated z^* value was about three times the canopy height.

2.7 Data processing

2.7.1 *Ramp parameters.* Determination of parameter γ in Eq.(A5) requires high frequencies measurements, especially for low and moderate canopy heights and, consequently, raw data needs to be recorded for post processing. Chen et al. [1997b] found that parameter γ is rather robust and constant for practical purposes. Table A.1 shows different mean parameter γ for a variety of canopies. According to Table A.1, as a rule of thumb, the parameter γ was set to, 1.1, for the low canopies (grass, rangeland grass, wheat and grapevines) and to 1.0 for nectarine and olive orchards. In general, the best time-lags (r_x) to solve Eq. (A5) were 0.2 s and 0.3 s, for the low canopies, 0.5 s and 0.75 s for the nectarine and olive orchards, respectively.

The sign of the ramp amplitude may be used to identify the stability conditions of the surface sub-layer. This is useful to select the correct form of the similarity functions $\phi_h(\zeta)$, $g_1(\zeta)$ and $g_2(\zeta)$ from temperature measurements taken at a single level without the need of extra measurements. However, near neutral conditions depending on the measurement frequency the sign of the ramp may not correspond with the measured sensible heat flux. For each canopy, the following number of failures (half-hourly samples) were obtained which includes all measurement heights; 64 over grass; 1027 over rangeland grass; 22 over grapevines; 25 over nectarines; and 259 over olives. For wheat all samples were in accordance because the experiment was carried out with relatively high H values. The failures were found within the following ranges for the stability parameter and sensible heat flux (in Wm^{-2}) values; ($-0.15<\zeta<0.01$) and ($-18<H<7.5$) for grass; ($-0.02<\zeta<0.01$) and ($-9.0<H<9.0$) for rangeland grass; ($-0.05<\zeta<0.01$) and ($-8.1 <H< 12.3$) for nectarines; and ($-0.03<\zeta<0.02$) and ($-21.1 <H< 10.5$) for olives. Samples within those ranges were not included in the analysis. The number of data analysed are listed in Table 1.

2.7.2 *Temperature structure function parameter*. The second order structure function was employed to determine the temperature structure function parameter as $D^2(x) = C_{tt}\, x^{2/3}$, where $D^2_{(x)}$ *and* x denotes the second order structure function and the spatial separation between the two measurements of temperature, respectively (Stull, 1991). The Taylor hypothesis of frozen turbulence can be used to convert time series into spatial series as $S^2(r) = C_{tt}\, (\bar{u}\, r)^{2/3}$, where $S^2_{(r)}$ and r were defined in (A1 for n=2) and $\bar{u}$ denotes the mean wind speed along the flow direction. The Taylor's frozen hypothesis was used to convert time-lags into stream-wise distances using horizontal wind speeds measured with a 3D-sonic anemometer during experiments over grass in year 2001 and the rangeland grass. When 3D-sonic measurements were unavailable the cup anemometer measurements were corrected at different levels using the wind-profile law, experiments over grass in 1994 and 1995.

2.7.3 *Stability parameter and sensible heat flux.*

After determining the required input for the corresponding equation to estimate sensible heat flux (temperature ramp parameters, standard deviation, third order structure function and structure function parameter), one must determine the stability parameter unless a free-convection limit approach is used. When, the data required for determining the Obukhov length is unavailable, iteration or optimization methods are used. Iteration based on the wind-profile law (Brutsaert,1982) solves for convergence of the conjunction of friction velocity, stability parameter, and sensible heat flux by starting the iteration process assuming neutral conditions. This procedure was implemented for the experiments over grass in years 1994 and 1995, wheat, and grapevines. A description can be found in Castellví et al.[2002] and Castellví [2004]. For the experiments over grass in year 2001 and rangeland grass the measured air temperature, friction velocity and sensible heat flux were used for determining the stability parameter.

For the olive orchard, horizontal wind speed was available at a single level close to the canopy top and, therefore, wind-profile law was not applicable. Friction velocity was estimated using the measured horizontal wind speed at the canopy top [Kaimal and Finnigan, 1994]. Simulating annealing procedure in conjunction with the Metropolis criteria was used for stability parameter and sensible heat flux optimization. Details about the procedure can be found in Castellvi and Martínez-Cob [2005].

For the nectarine orchard experiment, the friction velocity, stability parameter, and horizontal wind speed above the canopy were unavailable. Therefore, friction velocity was estimated as follows. Under unstable atmospheric conditions, the scale $\lambda^*_{(\zeta)}$ was used (Appendix B): $u_* \approx z/[\tau\, \lambda^*_{(\zeta)}] \approx z/[\tau\, 0.75^3]$. Also, the friction velocity was estimated using the following relationship [Stull, 1991]: $u_* \approx [\langle w'^2\rangle/1.7]^{0.5}$ where $\langle w'^2\rangle$ is the variance of the vertical wind velocity that was recorded each half hour. Under stable atmospheric conditions, friction velocity was estimated using only $u_* \approx [\langle w'^2\rangle/1.7]^{0.5}$ because the scale $\lambda^*_{(\zeta)}$ was uncertain. The stability parameter was obtained from the Obukhov length using the corresponding estimated u_* and the measured sensible heat flux.

3. RESULTS

The performance of Eq.(8) for estimating friction velocity and the new and existing equations for estimating sensible heat flux was analysed in terms of linear regression analysis, where the measured values were taken as the independent variable, coefficient of determination, R^2, and the root mean square error, RMSE. When calibration is not possible, RMSE indicates the accuracy of the model. However, the RMSE values were also analysed in terms of systematic, RMSEs, and unsystematic, RMSEu, parts (see glossary). According to Willmott [1982], $RMSE^2 = RMSEu^2 + RMSEs^2$. Consequently, the portion of the systematic errors presumably contained in the model, SE (expressed in %), can be described by $SE=100\ RMSEs^2/\ RMSE^2$. When SE is high, it is possible to dampen a new parameterization of the model without making significant changes in model's structure. Therefore, the expression UE = 100 - SE can be interpreted as a measure of potential accuracy improvement. Assuming possible model calibration, UE represents the $RMSE^2$ portion that the model cannot explain. In such case, for a given RMSE, the accuracy can be evaluated by UE (i.e., the lower UE, the higher the accuracy). On the other hand, when the RMSE is small enough, indicating that the model is accurate and calibration is not needed, relatively high UE percentages may be expected.

3.1 Friction velocity

Table 2 lists the statistics obtained corresponding to the performance of Eq. (8) in estimating the friction velocity. It is shown the slope and intercept (in m s^{-1}) from a linear fitting, R^2, and the RMSE (m s^{-1}) and UE, for each measurement height, stability conditions and for the whole dataset for all canopies except for the nectarine orchard because direct measurement was unavailable. In general, whatever the measurement level and stability conditions, including homogeneous and heterogeneous canopies, the intercepts were negligible, R^2 values were high, and the RMSE values were small. Consequently, improvements over the Eq.(8) estimates are unlikely (UE percentages were relatively-high) because it did a good performance.

3.1.1 *Measurements taken in the inertial sub-layer*. In the experiments over grass and rangeland grass, performance was generally excellent regardless of the stability conditions.

Under unstable conditions, measurements collected up to 1 m revealed a consistent overestimation on the order of 15%. For these cases, the highest UE value was obtained over grass at level of 1.5 m height, UE =82%. At this level, a calibration factor would slightly improve the RMSE because it was small, RMSE=0.02 m s^{-1}, indicating that Eq.(8) was sufficiently accurate and, therefore, there would not need modifications. For the 2.0 m level over rangeland grass, the RMSE obtained was the same as for the 1.5 m level over grass, but with a UE=53%, indicating that calibration would improve accuracy. The difference was related to the rangeland grass Eq. (8) being able to mostly capture the full measured friction velocity variability. For the 1.2 m and 1.3 m levels over grass, UE values indicate that a calibration factor would improve the RMSE (i.e., slopes departed considerably from one, 29% and 19 %). This overestimation, apart of a higher loss of covariance with height by the eddy covariance, was attributed to the measurement level being too far above the canopy. Entrainment of air from above likely contaminated the air temperature traces, which explains the substantial reduction in R^2 relative to lower levels, 0.7 m, 0.9 m and 1.0 m. The 0.6 m level also performed poorly relative to the 0.7 m, 0.9 m and 1.0 m. It was probably too close to the surface and it required a higher measurement frequency.

Under stable conditions, over grass UE was 46% indicating that the RMSE (0.04 m s^{-1}) can be substantially reduced. Calibration correcting the intercept would reduce the systematic error giving a RMSE of 0.02 m s^{-1}. For rangeland grass the RMSE=0.02 m s^{-1} was small, indicating no need for calibration (UE was 80%) despite its 9% underestimation.

3.1.2 *Measurements taken in the roughness sub-layer.* Table 2 shows that over wheat, the performance was good. For the upper level (1.3 m), the statistics listed in Table 2 were determined assuming that measurements occurred within the roughness and inertial sub-layers. The results were better when it was assumed that the data were collected in the roughness rather than the inertial sub-layer For the inertial sub-layer, there was an underestimation up to 25% and the UE=3% was small, indicating that most RMSE was systematic. This issue suggested a deep roughness sub-layer as was estimated. The lower accuracy was obtained when measuring at the canopy top and a higher measurement frequency would likely improve accuracy. For the 1.0 m level, calibrating the 2% overestimation would reduce the RMSE (UE=54%), but calibration was unnecessary for the 1.3 m level having RMSE=0.01 m s^{-1}, with UE= 91%. For all measurement levels, Eq. (8)

had an underestimation of 10% that could be corrected (slope of one) by increasing the roughness sub-layer depth to 2.85 times the canopy height.

For the grapevine experiment, Eq. (8) generally overestimated by around 13% at all measurement levels. Performance was excellent for the olive orchard regardless of the stability conditions and measurement level, although the highest level was slightly more accurate. For these two canopies, the low UE values obtained for all levels indicate that a calibration factor would substantially improve the estimates. This issue indicates that Eq.(8) could be very accurate if all the canopy and ramp parameters (z^*, d and γ) were accurately determined. Note that these parameters only affect the slope value, which implies a systematic error. The canopy morphology for grapevines was more complex than for the others and, therefore, a bigger error in estimating z^*, d and γ was expected.

For a variety of canopies, Eq. (8) performed well under stable and unstable conditions either when measuring close to or well above the canopy top. In general, the RMSE values were small. This is an indication that Eq. (8) was robust and eliminates the need for calibration. Figure 1 shows friction velocity estimates resulting from use of Eq. (8) for the entire data set including the six canopies.

3.2 Sensible heat flux

3.2.1 *Measurements taken in the inertial sub-layer.* Table 3 shows the slope and intercept (W m^{-2}) and R^2 determined by linear regression analysis, the RMSE (W m^{-2}) and UE (%) by measurement level and for all heights to show the performance of Eqs. (6), (13), (14), (21), (22) and of their respective free convection limit approaches, Eqs. (20), (18), (19), (23) and (24) for the experiments over grasses.

<u>*Unstable conditions*</u>. For the turf grass experiments all ten equations performed well. In general, the slope and R^2 values were close to one, and the intercept and RMSE values were small. For equations requiring air temperature and wind speed measurements, the maximum RMSE value obtained was RMSE=19.9 W m^{-2}, corresponding to Eq. (14) at the 1.5 m measurement level. For the free convection limit approaches, the maximum RMSE value obtained was RMSE=39.5 W m^{-2}, corresponding to Eq. (21) at the 1.5 m measurement level.

All the other cases had RMSE values below 25 W m^{-2}, which is the expected error for and eddy covariance system [Paw U et al., 1995]. Therefore, the performance was comparable to the eddy covariance system. Most UE percentages were high, indicating little room for improvement. These results suggest that for a similar experiment measuring within the adjusted surface layer, additional measurements for calibration of the equations is unnecessary.

For the 1.5 m level, Eq. (23) was not able to capture most of the measured H variability as well as the other equations, which require only temperature data. This was likely a consequence that the free convection limit for (21) holds for a narrower range of the stability parameter (ζ<-0.14) than it does for the other equations. For this level, Eq.(23) performed poorly, mainly for the range $-0.28 \leq \zeta \leq 0$. The R^2=0.04 using Eq.(23). The 1.5 m level experiment was conducted on the same plot but in a different year than the 1.3 m level experiment. Therefore, there is not an abrupt change in performance between the 1.3 m and 1.5 m measurement levels. Also, experiments measuring at levels of 0.6 m, 0.9 m and 1.2 m, and at levels of 0.7 m, 1.0 m and 1.3 m were conducted in years 1994 and 1995, respectively. Whatever the equation, exclusively based or not on similarity principles, the measured H variability tended to be better captured for the lower than for the higher levels, thus suggesting air entrainment from aloft. For the same plot, this trend was also found in Snyder et al.[1996] for Eq. (1).

For the rangeland grass experiment under unstable conditions, the best performance for equations requiring air temperature and wind speed measurements was obtained using Equation (6). It performed comparable to the eddy covariance system, RMSE=26.1 W m^{-2}. The other SR-based equations also performed well. For equations depending on the temperature parameter structure function, the performance obtained from Eq. (13) was better than for (21). According to the UE percentages, calibration of Eq. (21) reduce the RMSE, but it was not required for Eq.(13). After calibrating Eq. (21), the new RMSE was 42.8 W m^{-2}, which is still higher than using Eq.(13) without correction, which gave a RMSE=33.6 W m^{-2}. For equations depending on the temperature standard deviation, the performance obtained from Eq. (14) was slightly better than for (22). For both equations the intercept was negligible with high R^2 values and low UE percentages indicating that slope correction after calibration would improve their performance. After correction, the equations gave RMSE=35.1 W m^{-2} for (14) and RMSE=36.5 W m^{-2} for (22).

For the free convection limit approaches, Eqs. (20), (18) and (19) were comparable. Their performance was excellent and comparable to their respective expressions requiring wind speed measurements as input. Equations (21) and (22), however, generally performed considerably better than their free convection approaches, Eqs. (23) and (24), respectively. The intercept and R^2 values for Eqs. (23) and (24) were good, but the slopes departed considerably from unity. The RMSE values obtained for (23) and (24) were 90.7 W m^{-2} and 131.2 W m^{-2}, respectively, but the low UE percentages obtained (23% an 14%, respectively) indicate that they have potential improvement. Previous site-specific calibration of their corresponding similarity relationships would substantially reduce the RMSE. This issue suggest that for this experiment, the new derived equations were less sensitive to the site-performance of $g_1(\zeta)$ and $g_2(\zeta)$ than those equations exclusively based on similarity. Equation (13) depends of the power -1/6 on $g_1(\zeta)$, but Eq. (21) on the power –3/4. Equation (14) depends of the power -1/3 on $g_2(\zeta)$, whereas Eq. (22) on the power –2/3.

Stable conditions. For the turf grass experiments, Eqs. (6), (13) and (14) performed well. The RMSE were small indicating that these three equations, especially Eq.(6), showed similar accuracy to the eddy covariance. The UE percentages obtained were relatively high indicating that calibration was not needed. For rangeland grass, all three equations gave similar results but poor accuracy. The slopes and intercepts were around 0.5 and 20 W m^{-2}, respectively, R^2 values were around 0.25, and most of the RMSE (up to 85%) was unsystematic.

For equations (21) and (22), the performance was poor for either for grass or rangeland grass. The flux variance method was uncorrelated. Fetch was adequate for the rangeland experiment, but the performance from all the equations was worse than for the grass experiment. For rangeland grass, the corresponding relationships in Eq. (14), $g_1(\zeta)$ and $g_2(\zeta)$, did not hold under stable conditions. This probably might have resulted as a consequence of cool air drainage during night-time.

3.2.2 *Measurements taken in the roughness sub-layer*. Table 4 shows the slope and intercept (W m^{-2}) obtained by linear regression analysis, the R^2, the RMSE (W m^{-2}) and UE values corresponding to Eqs. (6) and (17), and for their respective free convection limit approach, Eqs. (20) and (19), for each measurement level and for the whole data set from experiments over wheat, grapevines, and nectarine and olive orchards.

Wheat experiment. As with the friction velocity estimates, H estimates were better at the 1.3 m level when it was assumed that the measurement level was located in the roughness sub-layer. When all equations were applied in the inertial sub-layer, most of the RMSE portion was systematic, the UE ranged from 4% to 14%. When all equations were applied assuming data collection within the roughness sub-layer, the slopes were close to one ranging from 0.9 to 1.08, and the intercepts were generally negligible regardless of the measurement height. The UE percentages were high, indicating that the improvement of these equations was potentially comparable and that most of the RMSE error was unsystematic because the equations were not able to fully capture the measured sensible heat flux variability. The R^2 values ranged from 0.66 to 0.82. Calibration would only slightly improve the RMSE values. The RMSE values, however, were reasonably good in all cases. According to RMSE values, Eq. (17) had slightly better performance than (6). This was also observed for their free convection limit approaches using Eqs. (19) and (20), respectively.

Grapevines experiment. Equation (6) had excellent performance for all levels. The slopes and R^2 values were close to one and the intercept and RMSE values were small. As a consequence, the UE were generally high, indicating that calibration of Eq. (6) was already unnecessary. Equation (17) gave biased results for all levels, but it was able to capture most of the measured H variability. Although the performance improved with the measurement height, the low UE values indicate that calibration to correct the bias for the higher levels (2.6m and 2.9m) and, both bias and slope for the lower levels (2.0 m and 2.3 m) would substantially improve the accuracy. It is not shown in Table 4, but after calibration, Eq.(17) performed similar to Eq.(6).

The corresponding free convection limits approaches for Eq. (6) and (17), Eq. (20) and (19) respectively, had slopes close to 1.0 for all the levels but gave more biased results, especially Eq.(19) with lower R^2 values. Equations (20) and (19) had small UE percentages, indicating that correction of the bias would greatly reduce the RMSE. It is not shown in

Table 4, but Eq. (20) performed better than (19) even after correction of Eq.(19). Apart of the general overestimation resulting from use of Eq. (8), which is clearly observed in Eq. (17), the assumption made in Eq.(18) could be rather unrealistic for this heterogeneous canopy. This may explain the different performance obtained between Eq. (6) and (17) and for their free convection limit approaches. Assuming that calibration is not possible, the RMSE values from Eq. (20) were reasonable for all the levels, and therefore more attractive than Eq. (19). Overall, Eq. (6) performed better than (17). The same was observed for their free convection limit approaches.

Nectarine orchard experiment. Under unstable conditions, Equation (6) showed excellent performance regardless of the level and method used for estimating the friction velocity. The RMSE values obtained were small. The UE percentages were also low indicating that if bias were corrected (slopes and R^2 values were close to one) the general performance would be close to the eddy covariance. Whether or not calibration was used, Eq. (6) was more accurate than (17) and it better represented the measured H variability. The RMSE values obtained using Eq. (17) were reasonably good, so it performed well for estimating H. The performance given by Eq. (6) was comparable to its free convection limit approach, Equation (20). This was not observed for Eqs. (17) and (19), with (19) being slightly more accurate than (17). It was likely a consequence of the inaccuracy involved into the similarity relationships operating at the canopy top.

Under stable conditions, Eqs. (6) and (17) had reasonably good performance. The RMSE values were good, but calibration would reduce the bias. Equation (6) was slightly better than (17). The R^2 values were low, however, for this experiment sensible heat fluxes were within a narrow range, $-47.3 \leq H \leq 0.0$ W m^{-2}, and most samples fell within the measurement error. This makes the interpretation of the statistics listed in Table 4 difficult.

Overall, regardless of the measurement level, the method for estimating the friction velocity and stability of the surface layer, Eqs.(6) and (20), which are based on ramp amplitude, performed slightly better than those based on the standard deviation, Eqs.(17) and (19).

Olive orchard experiment. Regardless of the measurement level or stability conditions, the equations performed well. The RMSE values obtained were small. The UE percentages for Eq.(6) were higher than for Eq.(17), probably because it was already more accurate. The same was observed for their free convection limit approaches All of the equations had small intercept values, but the slopes for Eqs. (17) and (19) could potentially improve with calibration. After calibration of Eqs. (17) and (19), the performance was similar to Eqs.(6) and (20). Therefore, although potentially comparable, the equations based on ramp amplitude resulted more reliable.

Overall results. For all crops analysed, all of the equations performed reasonably well. However, the equations based on ramp amplitude were in general more accurate. The fact that Eqs.(17) and (19) over wheat and the two orchards (nectarine and olive) showed good performance indicates that Eq.(18) gave realistic results for homogeneous and some heterogeneous canopies. It did not seem true for heterogeneous canopies, such as grapevines. To test the Eq.(18) performance over grapevines requires measurements which were unavailable.

3.2.3 *The flux-variance method.* Although mainly for Equation (24), the flux-variance method has also been tested under non-ideal field conditions. Equations (22) and (24) were analysed for the experiments over wheat and grapevines in Castellví [2004] and for the olive orchard in Castellví and Martínez-Cob [2005]. The results obtained indicate that new Eqs. (17) and (19), depending on the temperature standard deviation, were comparable or performed better than (22) and (24), respectively. For the olive orchard experiment, under stable atmospheric conditions, the flux-variance method was not applicable because the similarity relationship, $g_2(\zeta)$, was uncertain [Castellví and Martínez-Cob, 2005]. Equation (17), however, performed reasonably well (Table 4) indicating it was robust relative to (22) under conditions unfavourable to meeting similarity requirements. Equation (17) depends on $g_2(\zeta)$ less than (22).

For the nectarine orchard, the H estimates from Eqs. (22) and (24) were often poor for values of H less than 70 W m^{-2}. This indicated that close to the canopy $g_2(\zeta)$ held better when thermal convection becomes important (i.e., turbulence tends to be decoupled from the surface). Equations (17) and (19) were mostly superior to (22) and (24) for H values below 95 W m^{-2}. Under stable atmospheric conditions, Eq. (22) exhibited poor regression statistics, with slope, intercept and R^2 values of 0.42, -8.6 W m^{-2} and 0.07, respectively. The RMSE = 32.1 W m^{-2} and UE=91%, indicating that, even after calibration, Eq. (22) would be inferior.

Figure 2 shows H values obtained with Eqs. (13) and (14) over rangeland grass (Figures 2a and 2b), Eq. (19) for all the measurement heights over wheat and grapevines (Figures 2c and 2d), Eqs. (19) and (20) over nectarine orchard (Figure 2e), Eq. (17) over the olive orchard (Figure 2f). Figures showing the performance of Eq. (6) for the grass, wheat and grapevines are published in Castellví [2004]. Estimates from Eqs. (6), (20) and (22) over the olive orchard are provided by Castellví and Martínez-Cob [2005].

4. SUMMARY AND CONCLUDING REMARKS

Based on SR analysis and similarity principles, two new equations (13) and (14) for estimating sensible heat flux density when measurements are taken well above a canopy top were presented. The new equations are based on Eq. (8) for estimating friction velocity. Equation (8) was combined with three relationships that are valid for estimating the temperature scale (T_*) in the inertial sub-layer [Eqs. (9), (11) and (12)] giving Eqs. (13) and (14). Equation (13) depends on the parameter of the temperature structure function and (14) on the standard deviation of temperature. Their respective free-convection limits, Eqs. (18) and (19), exhibited a weak dependence on the stability parameter under slightly unstable conditions permitting sensible heat flux estimates from air temperature as the only input under unstable conditions. Equation (14) was modified for operating above but close to the canopy top, Eq. (17). The free convection limit for (17) also held for slightly unstable conditions, Eq. (19).

In general, when measuring well above the canopy top, the new equations showed excellent performance under unstable conditions. The results obtained suggest that Eqs. (13) and (14) and their respective free convection limit expressions provide a practical technique to use the SR analysis without the need for calibration. Equations (17) and (19) appear even robust when measurements are made over rather heterogeneous canopies (nectarine and olive orchards). The results were biased, however, for a very heterogeneous canopy (grapevines). The new equations are less sensitive to similarity functions than are equations (21) and (22) which are exclusively based on similarity principles. This is convenient since similarity function may require site-specific calibration when similarity requirements are not fully met such as when measuring over growing vegetation or close to the canopy. Measuring close to the canopy top reduces fetch requirements and the need for tall micrometeorological towers, making the campaigns more affordable.

Under stable conditions, the combined SR-similarity equations are superior to the exclusively similarity-based Eqs. (21) and (22). The similarity functions performance, however, still played a key role. This explain why Eq.(6) showed the best performance.

In conclusion, it was shown that the equations obtained as a result of combining SR analysis and similarity principles are more robust than those based solely on similarity either when measuring well above or close to the canopy top and over non-homogeneous canopies. Equation (6) and its free convection limit generally performed best. Equation (19) appeared attractive for field applications. It performed well and permits affordable battery-powered data loggers to record temperature and compute sensible heat flux density on–line.

5. ACKNOWLEDGMENTS

We gratefully acknowledge K.T Paw U, the associate editor and three reviewers for their useful, constructive and competent suggestions. We thank Asun and Carla for their assistance, D. Spano for the experiments over grass, wheat and grapevines, I. Ferreira for supporting the collection of data over the nectarine orchard in Portugal, J. Faci, M. Izquierdo, J. Gaudó and D. Mayoral for their field assistance for the olive orchard experiment, and the owner of this orchard for his allowance of the experiment. We also thank the University of California, Davis for providing facilities to analyse the data. This work was supported by the Ministerio de Ciencia y Tecnología under the Spanish project REN2001-1630 CLI, the DURSI of the Generalitat of Catalunya and the University of Lleida. Data from the grassland was supported by grants from the US Dept of Energy and the California Agricultural Experiment Station.

6. REFERENCES

Albertson, J.D., M.B. Parlange, G. Katul, C.R. Chu, H. Striker, and S. Tyler (1995), Sensible heat flux estimates using variance methods, *Water Resour. Res.*, *31*(4), 969-974.

Allen, R.G., L.S. Pereira, D. Raes, M. Smith (1998). Crop evapotranspiration: guidelines for computing crop water requirements. FAO *Irrigation and Drainage* Paper Nº 56. FAO, Rome, Italy, 300 pp.

Allen, R.G., W.O. Pruitt, J.A. Businger, L.J. Fritschen, M.E. Jensen, and F.H. Quinn (1996), Evaporation and Transpiration, in: *Hydrology Handbook*, 2nd ed., ASCE Manual and Reports on Engineering Practice No. 28, overall editing by. R.J. Heggen, Task Committee Members, T.P. Wootton, C.B. Cecilio, L.C. Fowler, S.L. Hui, pp. 125-252, *American Society of Civil Engineers*, New York.

Anderson, F.E., R.L. Snyder, R.L. Miller and J. Drexler (2003), A micrometeorological investigation of a restored California wetland ecosystem. *B. Am. Meteorol. Soc*., 84, 9, 1170-1172.

Antonia, R.A., A.J. Chambers and E.F., Bradley (1981). Temperature structure in the atmospheric surface layer II. The budget of mean cube fluctuations. *Bound-Lay. Meteorol.*, *20*, 293-307.

Baldocchi, D.D., Liukang, X., and Kiang N., 2004. How plant functional-type, weather, seasonal drought, and soil physical properties alter water and energy fluxes of an oak-grass savanna and an annual grassland. *Agric. Forest Meteorol*., 123: 13-39.

Brutsaert, W. (1982), Evaporation into the atmosphere, 299 pp., D. Reidel P.C., Dordrecht, The Netherlands.

Businger, J.A., J.C. Wyngaard, I. Izumi, and E.F. Bradley (1971), Flux profile relationships in the atmospheric surface layer, *J. Atmos. Sci.*, *28*, 181-189.

Castellví, F., P.J. Perez, and M. Ibañez (2002), A method based on high-frequency temperature measurements to estimate the sensible heat flux avoiding the height dependence, *Water Resour. Res.*, *38*(6), 1084, DOI: 10.1029/2001WR000486.

Castellví, F. (2004), Combining surface renewal analysis and similarity theory: A new approach for estimating sensible heat flux, *Water Resour. Res.*, *40*, W05201, DOI:10.1029/2003WR002677.

Castellví, F. and Martínez-Cob (2005), Estimating sensible heat flux using surface renewal analysis and the variance method. A study case over olive trees at Sástago (NE, Spain). *Water Resour. Res.*, 41, 9, W0942, DOI:10.1029/2005WR004035.

Cellier, P. (1986), On the validity of flux-gradient relationships above very rotugh surfaces, *Bound-Lay. Meteorol.*, *36*, 417-419.

Cellier, P., and Y. Brunet (1992), Flux-gradient relationships above tall plant canopies, *Agr. Forest Meteorol.*, *58*, 93-117.

Chen, W., M.D. Novak, T.A. Black, and X. Lee (1997a), Coherent eddies and temperature structure functions for three contrasting surfaces. Part I: Ramp model with finite micro-front time, *Bound-Lay. Meteorol.*, *84*, 99-123.

Chen, W., M.D. Novak, T.A. Black, and X. Lee (1997b), Coherent eddies and temperature structure functions for three contrasting surfaces. Part II: Renewal model for sensible heat flux, *Bound-Lay. Meteorol.*, *84*, 125-147.

De Bruin, H.A.R., W. Kohsiek, and B.J.J.M. Van Den Hurk (1993), A verification of some methods to determine the fluxes of momentum, sensible heat and water vapor using standard deviation and structure parameter of scalar meteorological quantities, *Bound-Lay. Meteorol.*, *63*, 231-257.

De Bruin, H.A.R., N.J. Bink, and L.J.M. Kroon (1991), Fluxes in the surface layer under advective conditions, edited by T.J. Schmugge and J.C. André, pp. 157-171.

Duce, P., D. Spano, and R.L Snyder (1998). Effect of different fine-wire thermocouple design on high frequency temperature measurements. AMS 23rd Conf. On Agricultural and Forest Meteorol., Alburqueque, NM, 146-147.

Gao, W., R. H. Shaw and K. T. Paw U (1989), Observation of organized structure in turbulent flow within and above a forest canopy, *Boundary-Lay. Meteorol., 47*, 349-377.

Garrat, J.R. (1980), Surface influence upon vertical profiles in the atmospheric near-surface layer. *Q.J.R.Meteorol. Soc*., *10*6, 803-819.

Higbie, R. (1935), The Rate of Absorption of a Pure Gas into a Still Liquid during Short Periods of Exposure, *Trans. Am. Inst. Chem. Engr., 31*, 365-388.

Högström, U. (1990), Analysis of turbulent structure in the surface layer with a modified similarity formulation of near neutral conditions, *J. Atmos. Sci.*, *47*, 1949-1972.

Hsieh, C., and G. Katul (1996), Estimation of momentum and heat fluxes using dissipation and flux-variance methods in the unstable surface layer, *Water Resour. Res.*, *32*(8), 2453-2462.

Kader B.A., and A.M. Yaglom (1990), Mean fields and fluctuation moments in unstably stratified turbulent boundary layers, *J. Fluid Mech.*, *212*, 637-662.

Kaimal, J.C, and J.J. Finnigan (1994), *Atmospheric Boundary Layer Flows, their Structure and Measurement*, 289 pp., Oxford Univ. Press, New York.

Katul, G., M. Goltz, C. Hsieh, Y. Cheng, F. Mowry, and J. Sigmon (1995), Estimation of surface heat and momentum fluxes using the flux-variance method above uniform and non-uniform terrain, *Bound-Lay. Meteorol.*, *74*, 237-260.

Katul, G., C. Hsieh, R. Oren, D. Ellsworth, and N. Philips (1996), Latent and sensible heat flux predictions from a uniform pine forest using surface renewal and flux variance methods, *Bound-Lay. Meteorol.*, *80*, 249-282.

Kormann, R., and F.X. Meixner (2001), An analytical footprint model for non-neutral stratification, *Bound-Lay. Meteorol., 99,* 207-224.

Kustas, W.P., J.R. Prueger, K.S. Humes, and P.J. Starks (1999), Estimation of surface heat fluxes at field scale using surface layer versus mixed layer atmospheric variables with radiometric temperature observation, *J. Appl. Meteorol., 38*, 224-238.

Lloyd, C.R., A.D. Culf, A.J. Dolman, and J.H.C. Gash (1991), Estimates of heat flux from observations of temperature observations, *Bound-Lay. Meteorol.*, *57*, 311-322.

Montheith, J.L, and M.H. Unsworth (1990), Principles of environmental physics, (Second edition), pp-291, Ed. Routledge, New York (NY, USA).

Padro, J. (1993), An investigation of flux-variance methods and universal functions applied to three land-use types in unstable conditions, *Bound-Lay. Meteorol.*, *66*, 413-425.

Paw U, K. T., Y. Brunet, S. Collineau, R.H. Shaw, T. Maitani, J. Qiu, and L. Hipps (1992), On coherent structures in turbulence within and above agricultural plant canopies, *Agric. Forest Meteorol., 61*, 55-68.

Paw U, K.T., J. Qiu, H.B. Su, T. Watanabe, and Y. Brunet (1995), Surface renewal analysis: a new method to obtain scalar fluxes without velocity data, *Agr. Forest Meteorol.*, *74*, 119-137.

Paw U, K.T., R.L Snyder, D. Spano, and H.B. Su (2005), Surface renewal estimates of scalar exchanges, *Micrometeorology in Agricultural Systems, Agronomy Monograph 47, Chapter 20*, ASA-CSSA-SSSA Publishers, Madison (Wi, USA).

Qiu, J., K.T. Paw U, and R.H. Shaw (1995), Pseudo-Wavelet analysis of turbulence patterns in three vegetation layers, *Boundary-Lay. Meteorol., 72*, 177-204.

Raupach, M.R, J.J. Finnigan, and Y. Brunet (1996), Coherent eddies and turbulence in vegetation canopies: the mixing-layer analogy. *Boundary- Lay. Meteorol.*, *78*, 351-382.

Sellers, P.J., Y. Mintz, Y.C. Sud and A. Dalcher (1986), A simple biosphere model (SiB) for use within general circulation models, *J. Atmos. Sci., 43*, 505-531.

Shaw, R.H., Y. Brunet, J.J. Finnigan, M.R. Raupach (1995), A wind tunnel study of air fow in waving wheat: Two-Point velocity statistics, *Boundary-Lay. Meteorol. 76*, 349-376.

Shaw, R.H. (2002), Flow above and within the canopy. *Lecture 20 in Advanced short course on agricultural, forest and micrometeorology*, pp-303, Consiglio Nazionale delle Ricerche, Sassari (Italy).

Snyder, R., D. Spano and K.T. Paw U (1996), Surface renewal analysis for sensible and latent heat flux density, *Boundary-Lay. Meteorol., 77*, 249-266.

Spano, D., R.L. Snyder, P. Duce and K.T. Paw U (1997), Surface renewal analysis for sensible heat flux density using structure functions, *Agric. Forest Meteorol. 86*, 259-271.

Spano, D., R.L. Snyder and K.T. Paw U (2000), Estimating sensible and latent heat flux densities from grapevine canopies using surface renewal, *Agric. Forest Meteorol., 104*, 171-183.

Stull, R.B. (1991), *An Introduction to Boundary Layer Meteorology*, 666 pp., Kluwer Acad. Publishers, Dordrecht, The Netherlands.

Tillman, J.E. (1972)., The indirect determination of stability, heat and momentum fluxes in the Atmospheric boundary layer from simple scalar variables during dry unstable conditions, *J. Appl. Meteorol.*, *11*, 783-792.

Twine, T.E., W.P. Kustas, J.M. Norman, D.R. Cook, P.R. Houser, T. P.Meyers, J.H. Prueger, P.J. Starks, and M.L. Wesely (2000), Correcting eddy-covariance flux underestimates over a grassland, *Agr. Forest Meteorol*., 103, 279-300.

Van Atta, C. W. (1977), Effect of coherent structures on structure functions of temperature in the atmospheric boundary layer, *Arch. of Mech., 29*, 161-171.

Weaver, H.L. (1990), Temperature and humidity flux-variance relations determined by one-dimensional eddy correlation, *Boundary-Lay. Meteorol., 53,* 77-91.

Wesely, M. (1988), Use of variance techniques to measure dry air-surface exchange rates, *Bound-Lay. Meteorol.*, *44*, 13-31.

Wesson, K.H, G. Katul, and Chun-Ta Lai (2001), Sensible heat flux estimation by flux variance and half-order time derivative methods, *Water Resour. Res.*, *37*(9), 2333-2343.

Willmott C.J. (1982), Some comments on the evaluation of model performance. *Bulletin American Meteorological Society. 63 (11)*, 1309-1313.

Wyngaard, J.C., Y. Izumi and S.A. Collins (1971), Behavior of the Refractive-Index Structure Parameter near the Ground, *J. Opt. Soc. Am.*, *61*, 1646-1650.

Zapata, N., and A. Martínez-Cob (2001), Estimation of sensible and latent heat flux from natural sparse vegetation surfaces using surface renewal, *Journal of Hydrol.*, *254*, 215-228.

7. APPENDIX A. Ramp parameters.

Structure functions, Eq. (A1), and the analysis technique, Eqs. (A2) to (A4), from Van Atta (1977) were used to determine ramp amplitude, *A*:

$$S^n(r) = \frac{1}{m-j}\sum_{i=1+j}^{m}\left(T_i - T_{i-j}\right)^n \qquad \text{(A1)}$$

where *m* is the number of data points in the 30-minute interval measured at frequency (*f*), *n* is the power of the function, *j* is a sample lag between data points corresponding to a time-lag (r=*j/f*), and T_i is the ith temperature sample. An estimate of the mean value for *A* is determined by solving Eq. (A2) for the real roots

$$A^3 + pA + q = 0 \qquad \text{(A2)}$$

where

$$p = 10S^2(r) - \frac{S^5(r)}{S^3(r)} \qquad \text{(A3)}$$

and

$$q = 10S^3(r) \qquad \text{(A4)}$$

According to ramp-scheme in Figure A1, the relationship between the inverse ramp frequency ($\tau=L_r+L_f$) and ramp amplitude is [Chen et al. 1997a]

$$\frac{A}{\tau^{1/3}} = -\gamma\left(\frac{S^3(r_x)}{r_x}\right)^{1/3} \qquad \text{(A5)}$$

where r_x is the time lag r that maximizes (S^3(r)/r) and γ is a parameter that corrects for the difference between $A/\tau^{1/}3$ and $(S^3(r)/r)^{1/3}$ evaluated at r_x. Parameter γ varies by less than 25% with respect to unity, (0.9-1.2) for the range of canopies in table A1. For bare soil and straw mulch parameter γ mainly varies between (1 and 1.2), while for Douglas-fir Forest it mainly varies between (0.9 and 1.1). Mean values for parameters γ and r_x and the suitable measurement frequencies, Hz, required for different canopies to solve A5 (i.e. to capture the appropriate solution to A5 for most samples) are shown in Table A1.

Table A1. Recommended mean values for γ, r_x (s) and sampling frequencies (Hz) for different canopies [Chen et al., 1997a].

Canopy height	γ	Hz	r_x
Fir Forest, 16.7 m	1.001	5	0.833
Straw Mulch, 0.06 m	1.175	11	0.111
Bare Soil	1.104	26	0.066

8. APPENDIX B. Analysing the atmospheric stability dependence for estimating sensible heat flux from Eqs. (13), (14) and (17).from air temperature measurements

The dependence on the stability parameter corresponding to the functions: $\phi^{-3/5}{}_{h}(\zeta)/(-\zeta)^{1/5}$ in Eq.(6), $\phi^{-2/3}{}_{h}(\zeta)\ g_{1}{}^{-1/6}(\zeta)/(-\zeta)^{1/3}$ in Eq.(15) and $\phi^{-2/3}{}_{h}(\zeta)\ g_{2}{}^{-1/3}(\zeta)/(-\zeta)^{1/3}$ in Eqs.(16) and (19) is shown in Figure 2B. Note that, as $S^{3}{}_{(rx)}$ is positive under stable conditions (Fig. 2B) these functions are represented taking ζ instead of -ζ as being consistent with the sign of sensible heat flux (H positive upwards). All functions show similar trends with respect to the stability parameter, regardless of the stability conditions. Under unstable conditions, the three equations present absolute minimum values with a weak dependence on the stability parameter for a wide range of unstable conditions. This allows us to approximate the stability functions in Figure 2B as constant. Reasonable relative errors are introduced in the range $\zeta \leq -0.01$ when the functions in Figure 2B corresponding to Eqs. (6), (15), (16) and (19) are approximated as constants with values of 2.4 (see equation 7), 2.6 and 2.6, respectively. For example, when the stability parameter ranges between the intervals: $-0.1 \leq \zeta \leq -0.01$, $-0.75 \leq \zeta \leq -0.1$, and $-2 \leq \zeta \leq -0.75$, the corresponding respective mean relative errors obtained by this assumption are: 3.2%, 4.9% and 1.7% for Eq. (6), 14.6%, 4.7% and 0.4% for Eq. (15) and 14.2%, 3.2% and 5.7% for Eq. (16) or (19), respectively. Under stable conditions the corresponding functions are highly dependent on the stability parameter producing large errors if a constant is set to avoid dependence upon the stability parameter.

Combining Eqs.(3) and (4), the following expression for parameter $[\alpha(k\beta)^{2}]^{1/3}$ is obtained

$$\left[\alpha\ (k\beta)^{2}\right]^{1/3} = \begin{cases} \left(\dfrac{k}{\pi}\right)^{1/2}\left(\dfrac{(z-d)}{z^{2/3}}\right)^{1/2}\left(\dfrac{\phi_{h}(\varsigma)}{\tau u_{*}}\right)^{1/6} & z > z^{*} \\ \left(\dfrac{k}{\pi}\right)^{1/2}\dfrac{z^{2/3}}{(z^{*})^{1/2}}\left(\dfrac{\phi_{h}(\varsigma)}{\tau u_{*}}\right)^{1/6} & h \leq z \leq z^{*} \end{cases} \qquad \text{(B1)}$$

For a wide range of surface layer atmospheric conditions, Eq. (B1) is weakly dependent on the stability parameter through the stability function for heat due to its 1/6 power dependence. Based on ramp frequency scales with wind shear, Chen et al. [1997b] scaled $1/(\tau u_{*})$ over z or $(z-d)$ in the roughness and inertial sub-layers, respectively, through a constant parameter, λ. Here, the scale to analyse Eq. (B1) was used as a generalized form depending on the stability parameter, $\lambda_{(\zeta)}$,

$$\left[\alpha\ (k\beta)^2\right]^{1/3} = \begin{cases} \left(\frac{k}{\pi}\right)^{1/2} \left(\frac{(z-d)}{z}\right)^{1/3} \left(\lambda(\varsigma)\ \phi_h(\varsigma)\right)^{1/6} & z > z^* \\ \left(\frac{k}{\pi}\right)^{1/2} \left(\frac{z}{z^*}\right)^{1/2} \left(\lambda^*(\varsigma)\ \phi_h(\varsigma)\right)^{1/6} & h \le z \le z^* \end{cases} \qquad \text{(B2)}$$

where parameters, $\lambda_{(\zeta)}=(z-d)/(\tau u_*)$ and $\lambda^*_{(\zeta)}=z/(\tau u_*)$, denote generalized scales corresponding for measurements made well above and close to the canopy, respectively. Hence, joining the performance of the functions shown in Figure 2B and the dependence of equation (21) on the stability parameter, it allows one to analyse the total dependence on the stability parameter corresponding to Eqs. (15), (16) and (19). This is shown in the results.

4.2 Analysing the dependence on the stability parameter of scales $\lambda_{(\zeta)}$ and $\lambda_{*(\zeta)}$, parameter $[\alpha(k\beta)^2]^{1/3}$ and sensible heat flux for equations (15), (16) and (19).

Figure B1 shows the scales $[\lambda_{(\zeta)}]^{1/3}$ and $[\lambda^*_{(\zeta)}]^{1/3}$ versus the stability parameter for each canopy and measurement levels, except for the nectarines campaign because the friction velocity was unavailable. Whether measurements were made well above or close to the canopy top, both scales were rather insensitive to the stability conditions. When approximating to neutral and stable conditions its value becomes uncertain. Regardless of the measurement height above the canopy and type of canopy and according to these experimental results, it is proposed to approximate these scales to a constant value of 0.75 under unstable conditions that corresponds to a rounded value for $\zeta \le -0.025$ (Fig. B1). When measuring close to the canopy top, Paw U et al. [1992] found the relationship: $1/\tau \sim a\ u_h/h$, where u_h is the wind speed at the canopy top with height h with $a \sim 0.11$ over different crops. Other values for $a \sim (0.11, 0.35)$ have also been reported depending on wind shear [Shaw et al., 1995; Raupach et al., 1996]. As a general rule, a reasonable relationship between friction velocity and wind speed measured in the roughness sub-layer is as follows: $u_* \sim u_h/3$ [Raupach et al., 1996], leading to the relationship for the scale, $\lambda^*_{(\zeta)}=h/(\tau u_*)\sim 3a \sim$ [0.33, 1.05]. Therefore, because $[\lambda^*_{(\zeta)}]^{1/3} \sim [0.69,1.0]$, this interval is consistent with the proposed value for the scale $[\lambda^*_{(\zeta)}]^{1/3}$. Chen et al.[1997b] assumed the scale $\lambda^*_{(\zeta)}$ to be independent of ζ, $\lambda^*_{(\zeta)}=\lambda^*$ and, from linear fit analysis, they obtained λ^* values of 0.4, 0.54 and 0.70, respectively, from data collected over bare soil at 0.03 m, straw mulch (0.06 m thick) at 0.09 m and Douglas-fir Forest (16.7 m high) at 23 m. Therefore, the scale $[\lambda^*]^{1/3} \sim [0.73, 0.88]$, is also in agreement with the values shown in Figure B1.

Under unstable conditions, as a consequence of approximating the scales $\lambda_{(\zeta)}$ and $\lambda^*_{(\zeta)}$ as a constant from Eq. (B2), the dependence on the stability conditions attributed to the parameter $[\alpha(k\beta)^2]$ is through the relationship: $\phi^{1/2}{}_h(\zeta)$. Therefore, in Eq.(13) the total stability parameter sensible heat flux densities expressed as in Eq. (15) dependence ison the stability parameter through the stability function: $F_1(\zeta)= \phi^{-1/2}{}_h(\zeta)\ g_1{}^{-1/6}(\zeta)/(-\zeta)^{1/3}$. Similarly, sensible heat flux density from equations (14) and (17) have a dependence on the stability parameter through the function, $F_2(\zeta)= \phi^{-1/2}{}_h(\zeta)\ g_2{}^{-1/3}(\zeta)/(-\zeta)^{1/3}$. Figure B2 shows the dependence on the stability parameter on functions $F_1(\zeta)$ and $F_2(\zeta)$. They show similar pattern and a weak dependence on the stability parameter for a wide range of unstable conditions indicating that the corresponding free convection limit is achieved under slightly unstable conditions. Small relative errors are introduced when the stability parameters are approximated as constants with values $F_1(\zeta) \sim F_2(\zeta) \sim 2.2$. For example, when the stability parameter ranges in the interval, $\zeta \leq -0.1$, the respective mean relative errors obtained by this assumption are less than 10%. Equations (13), (14) and (17) may, therefore, provide good estimates of sensible heat flux density under unstable conditions and require only air temperature as an input.

Near neutral conditions, $F_1(\zeta)$ and $F_2(\zeta)$ sharply increase but Eqs. (13), (14) and (17) tend to zero as does the third order structure function. Under stable conditions, the stability functions $F_1(\zeta)$ and $F_2(\zeta)$ can also be approximated as constant for a wide range of the stability parameter: $1.0 \leq \zeta$. Figure B2 shows, however, that the stability functions are highly dependent on the stability parameter when $0 < \zeta \leq 1.0$. Such performance combined with the uncertainty of scales $\lambda_{(\zeta)}$ and $\lambda^*_{(\zeta)}$ This point out thea weakness for estimating sensible heat flux under stable conditions when only using air temperature measurements. as happened with equation (6). Under very stable conditions (e.g., $1.0 < \zeta$), relationships based on Monin-Obukov similarity ($\phi_h(\zeta)$, $g_1(\zeta)$ and $g_2(\zeta)$) may be uncertain [De Bruin et al., 1993]. It follows that Eqs. (13), (14) and (17) hold under moderate stable conditions and that wind speed as well as temperature measurements are required becausefor theirdetermining stability parameter dependence.

9. GLOSSARY OF SYMBOLS

A	Mean ramp amplitude.
C_p	Specific heat of air at constant pressure.
C_{tt}	Temperature structure function parameter.
d	Zero-plane displacement.
D	Mean free space between roughness elements
g	Acceleration due to gravity.
$g_1(\zeta)=\begin{bmatrix} 4.9(1-7\zeta)^{-2/3} & \zeta<0 \\ 4.9 & \zeta=0 \\ 4.9(1+2.75\xi) & \zeta>0 \end{bmatrix}$	Empirical similarity-based relationship (valid in the inertial sub-layer), Wyngaard et al. [1971].
$g_2(\zeta)=\begin{bmatrix} 0.95(0.05-\zeta)^{-1/3} & \zeta<0 \\ 2.5 & \zeta=0 \\ -2\,(uncertain) & \zeta>0 \end{bmatrix}$	Empirical similarity-based relationship (valid in the inertial sub-layer), Tillman [1972],
$g_2^*(\zeta)$	$g_2(\zeta)$ valid in the roughness sub-layer.
h	Canopy height.
H	Sensible heat flux.
Hec	Sensible heat flux measured with the eddy covariance.
k	Von Kármán constant.
K_h	Turbulent eddy diffusion for heat valid in the inertial sub-layer.
Kh^*	Turbulent eddy diffusion for heat valid in the roughness sub-layer.
L_0	Obukov length.
N	Number of observations.
r_x	Time lag that maximizes ($S^3(r)/r$).
$RMSE=\left[\dfrac{\sum_{i=1}^{N}(y_i-x_i)^2}{N}\right]^{1/2}$	Root mean square error.
$RMSEs=\left[\dfrac{\sum_{i=1}^{N}(\hat{y}_i-x_i)^2}{N}\right]^{1/2}$	Systematic root mean square error.
$RMSEu=\left[\dfrac{\sum_{i=1}^{N}(y_i-\hat{y}_i)^2}{N}\right]^{1/2}$	Unsystematic root mean square error.
R^2	Determination coefficient.
$S^n(r)$	Structure functions for *SR* analysis, Equation (A1).

T	Mean absolute air temperature.
T_*	Surface temperature scale.
UE	Unsystematic portion of RMSE^2.
u_*	Friction velocity.
x	Independent variable (measurement).
y	Dependent variable (estimate).
$\bar{y} = ax + b$	Predicted value (from the linear fitting $y = a + b\,x$) for the dependent variable.
z	Measurement height.
z^*	Roughness sub-layer depth.
α	Parameter in Equation (1).
β	Parameter in Equation (2).
$\phi_h(\zeta) = \begin{bmatrix} 0.74/\sqrt{1-9\zeta} & \zeta < 0 \\ 0.74 & \zeta = 0 \\ 0.74+5\zeta & \zeta > 0 \end{bmatrix}$	Stability function for heat transfer (valid in the inertial sub-layer), Businger et al. [1971].
$\phi^*_h(\zeta)$	Stability function for heat transfer (valid in the roughness sub-layer).
γ	Parameter in Equation (A5).
ρ	Air density.
σ_T	Temperature standard deviation.
τ	Mean inverse ramp frequency.
$\zeta = (z-d)/L_O$	Stability parameter.

FIGURE CAPTIONS

Figure A1. Ramp model with amplitude, A, and duration, τ, assuming a finite micro-front duration, L_f. The quiescent time period is neglected.

Figure B1. The scales $[\lambda_{(\zeta)}]^{1/3}$ and $[\lambda^*_{(\zeta)}]^{1/3}$ versus the stability parameter for: (*a*) grass; (*b*) wheat; (*c*) grapevines; (*d*) rangeland grass; and (e) olive orchard. All measurements heights.

Figure B2. Composed similarity functions, $F_1(\zeta)= \phi^{-1/2}{}_h(\zeta)\ g_1{}^{-1/6}(\zeta)/(-\zeta)^{1/3}$ in Eq.(13), and $F_2(\zeta)= \phi^{-1/2}{}_h(\zeta)\ g_2{}^{-1/3}(\zeta)/(-\zeta)^{1/3}$ in Eqs. (14) and (17) versus the stability parameter. Because $F_1(\zeta)$ and $F_2(\zeta)$ are undistinguishable, the function $F= F_1(\zeta)$ is shown.

Figure 1. Performance of Eq. (8) estimating friction velocity (m s^{-1}) over: (*a*) grass; (*b*) wheat; (*c*) grapevines; (*d*) rangeland grass; and (e) olive orchard, for all measurements heights. The 1:1 line is introduced for comparison.

Figure 2. Estimated versus measured with the eddy covariance, Hec (in W m^{-2}), sensible heat flux density over: (a) rangeland grass with Eq. (13); (*b*) rangeland grass with Eq. (14); (*c*) wheat; (*d*) grapevines using Eq. (19); (*e*) nectarine orchard using Eqs. (19) (circles) and (20) (triangles); and (f) olive orchard using Eq.(17). For all measurements heights. The 1:1 line is introduced for comparison.

Table 1. Summary of the experimental sites. Instruments: T, thermocouple measuring temperature at 8Hz; 1D, omni dimensional sonic anemometer measuring vertical wind speed at 10 Hz; 3D, three dimensional sonic anemometer measuring the wind components and virtual temperature at 10 Hz; CA, cup anemometer measuring half-hour wind speed.

Description		Exp. 1	Exp. 2	Exp. 3	Exp. 4	Exp. 5	Exp. 6
Surface		Grass	Wheat	Grape vineyard	Land grass	Nectarines	Olives
Location		Davis, CA	Davis, CA	Oakville, CA	Ione, CA	Portugal	Spain
Canopy height (m)		0.10	0.70	2.00	0.25	3.20	3.50
Homogeneous		Yes	Yes	No	Yes	No	No
Instrument heigth(m)	T	0.6 0.7 0.9 1.2 1.0 1.3	0.7 1.0 1.3	2.0 2.3 2.6 2.9		3.2	3.5 5.1
	1D	3D1.0 1.5CA	1.0	3.0		3.5	
	3D				2.0		4.9
	CA	2.0	2.0	3.0			
Fetch (m)		50	Sufficient	Sufficient	Sufficient	Sufficient	Sufficient
Range of H (W m^{-2})		-77 to 125	80 to 322	45 to 326	-78 to 473	-47 to 264	-98 to 416
Half-hour samples	Stable	261	-	-	2179	57	1887
	Unstable	317	43	133	3843	69	1907

TABLE 2. Performance of Eq. (8) for estimation of friction velocity. a, regression slope; b (m s^{-1}), intercept of regression (the measured friction velocity was the independent variable); R^2, coefficient of determination; RMSE (m s^{-1}), root mean square error; UE, unsystematic percentage of the mean square error (%).

Surface	Level (m)	Simple linear regression			Error statistics	
		b	a	R^2	RMSE (m s^{-1})	UE (%)
Grass (0.1 m tall)	0.6[u]	-0.01	1.09	0.72	0.03	75
	0.7[u]	0.00	1.00	0.90	0.01	82
	0.9[u]	0.01	1.01	0.89	0.03	66
	1.0[u]	0.04	0.94	0.91	0.01	46
	1.2[u]	-0.03	1.29	0.58	0.05	59
	1.3[u]	0.00	1.19	0.77	0.03	54
	1.5[u]	-0.03	1.13	0.91	0.02	82
	All levels[u]	0.00	1.07	0.85	0.02	59
	1.5[s]	0.02	1.03	0.82	0.04	46
Rangeland grass (0.25 m tall)	2.0[u]	0.01	1.13	0.96	0.02	53
	2.0[s]	0.01	0.91	0.81	0.02	80
Wheat (0.7 m tall)	0.7[u]	0.00	1.12	0.87	0.04	26
	1.0[u]	0.00	1.02	0.89	0.02	54
	1.3[u]	0.01	0.93	0.88	0.01	91
	All levels[u]	0.03	0.90	0.76	0.02	86
	1.3[u (a)]	0.01	0.73	0.88	0.05	3
Grape vineyard (2.0 m tall)	2.0[u]	0.00	1.17	0.98	0.08	8
	2.3[u]	0.01	1.14	0.99	0.08	20
	2.6[u]	0.01	1.11	0.98	0.07	34
	2.9[u]	0.02	1.11	0.98	0.07	18
	All levels[u]	0.01	1.13	0.98	0.08	19
Olive orchard (3.4 m tall)	3.5[u]	0.01	0.90	0.96	0.05	0
	5.1[u]	0.00	1.02	0.96	0.03	0
	All levels[u]	0.00	0.91	0.96	0.05	0
	3.5[s]	0.00	0.92	0.96	0.04	0
	5.1[s]	0.00	1.05	0.95	0.03	0
	All levels[s]	0.00	1.03	0.96	0.04	0

[u] Unstable conditions; [s] stable conditions.

[(a)] Estimates made assuming the level in the inertial sub-layer.

TABLE 3. Performance of Eqs. (6), (13), (14), (21) and (22) and their respective free convection limit approaches, Eqs. (20), (18), (19), (23) and (24), for estimation of H from measurements at the inertial sub-layer. a, regression slope; b, intercept of regression (W m^{-2}) (measured H, independent variable); R^2, determination coefficient; RMSE, root mean square error (W m^{-2}); UE, unsystematic percentage of the mean square error (%).

Grass (0.1m tall)																									
Equation:	(6)					(13)					(14)					(21)					(22)				
Level	a	b	R^2	RMSE	UE	a	b	R^2	RMSE	UE	a	b	R^2	RMSE	UE	a	b	R^2	RMSE	UE	a	b	R^2	RMSE	UE
0.6^u	0.96	0.2	0.97	5.3	92	1.07	-8.3	0.81	14.7	89	1.09	-8.2	0.80	14.8	91	1.10	4.7	0.85	11.6	93	1.15	4.1	0.85	11.8	76
0.7^u	0.97	-1.1	0.96	3.1	90	1.08	-4.8	0.84	3.8	48	1.10	-4.3	0.85	3.5	57	1.00	-0.6	0.98	0.3	88	0.99	-1.6	0.98	1.3	12
0.9^u	1.00	0.5	0.98	4.9	92	1.07	-8.1	0.88	11.8	86	1.09	-7.9	0.89	11.6	89	1.05	2.5	0.85	13.1	98	1.09	2.0	0 87	14.1	88
1.0^u	0.98	4.3	0.93	4.2	89	1.27	-11.9	0.83	5.5	19	1.29	-10.1	0.83	5.3	24	1.03	-0.4	0.50	4.4	95	1.01	–1.4	0.49	4.1	88
1.2^u	1.00	7.0	0.95	7.3	94	1.09	-11.1	0.85	15.7	84	1.11	-11.5	0.85	15.5	86	0.95	0.5	0.80	15.1	94	1.00	0.0	0.80	15.7	99
1.3^u	1.11	10.1	0.88	4.2	79	1.36	-13.2	0.76	6.2	38	1.39	-12.5	0.77	6.8	24	0.97	- 3.5	0.82	4.5	95	0.85	-4.5	0.82	4.4	94
1.5^u	0.97	5.7	0.83	12.9	87	1.01	18.2	0.53	19.3	79	1.04	17.2	0.51	19.9	78	0.86	-11.9	0.66	15.2	85	0.85	-10.5	0.65	17.3	77
All levels ^{u}	0.99	2.8	0.90	8.1	86	0.81	8.2	0.69	16.4	79	0.80	7.7	0.68	16.8	79	0.86	-5.5	0.77	14.7	87	1.01	-6.5	0.78	13.0	79
1.5^s	1.00	-7.7	0.85	3.9	85	0.92	3.2	0.46	9.5	71	1.14	5.2	0.42	13.2	70	0.70	-21.5	0.12	23.0	53	0.68	-25.8	0.00	29.5	31
Rangeland grass (0.25 m tall)																									
2.0^u	1.02	-10.1	0.95	26.1	96	0.98	2.3	0.95	33.6	95	0.87	1.1	0.92	38.2	53	0.87	-15.5	0.93	76.8	41	1.10	-5.1	0.93	49.5	39
2.0^s	0.56	-20.1	0.29	11.3	84	0.44	-17.5	0.22	13.1	87	0.47	-20.3	0.20	15.1	88	0.36	-9.5	0.12	14.1	97	0.30	-57.5	0.00	73.3	99
Grass (0.1m tall)																									
Equation:	(20)					(18)					(19)					(23)					(24)				
0.6^u	0.98	–8.6	0.81	15.3	78	0.93	-8.1	0.86	11.4	81	0.84	-7.2	0.86	11.7	38	1.10	5.5	0.78	23.4	23	0.87	7.2	0.73	21.9	44
0.7^u	1.04	-5.5	0.92	5.2	91	1.10	3.5	0.83	2.6	93	0.95	1.8	0.83	1.4	37	1.00	9.3	0.83	7.5	13	0.87	4.5	0.92	5.9	7
0.9^u	1.00	0.5	0.83	12.7	99	0.85	-7.9	0.90	8.3	81	0.90	-8.8	0.90	10.8	72	0.99	4.0	0.75	20.5	37	0.87	4.1	0.72	17.8	56
1.0^u	1.07	1.0	0.88	9.2	95	0.94	-1.2	0.83	2.3	95	0.96	-2.6	0.80	5.2	77	1.07	8.5	0.91	4.2	27	1.02	3.4	0.48	6.8	70
1.2^u	1.03	-0.2	0.78	15.7	99	0.91	-8.2	0.90	8.5	68	1.00	-10.6	0.90	15.6	37	0.95	3.3	0.79	18.1	46	0.81	2.1	0.73	17.5	55
1.3^u	1.17	11.2	0.77	7.7	21	0.86	–10.5	0.67	4.6	67	0.89	-14.4	0.59	13.8	84	0.86	4.5	0.82	4.2	58	0.85	-1.4	0.77	5.9	61
1.5^u	1.10	12.2	0.64	15.8	27	0.90	–16.4	0.75	15.0	62	0.86	-13.5	0.69	13.2	84	0.86	-32.0	0.04	39.5	82	1.14	-12.8	0.72	13.2	84
All levels ^{u}	1.01	4.6	0.72	16.4	85	1.02	-8.9	0.80	13.4	83	0.95	-8.6	0.80	11.8	73	0.83	-8.0	0.35	29.5	75	0.90	-3.7	0.77	12.3	87
Rangeland grass (0.25 m tall)																									
2.0^u	1.02	12.1	0.95	31.8	91	1.01	4.0	0.96	26.9	98	1.07	7.6	0.96	21.2	89	0.62	-1.1	0.88	90.7	23	1.37	17	0.93	131.2	14

^{u} unstable conditions; ^{s} stable conditions.

TABLE 4. Performance of Eqs. (6) and (17) and of their respective free convection limit approaches, Eqs. (20) and (19), in estimating H from measurements taken in the roughness sub-layer. It is shown the slope, a, intercepted, b (in W m^{-2}), from the linear fitting (the measured H was the independent variable), the determination coefficient, R^2, the root mean square error, RMSE (W m^{-2}) and its unsystematic portion, UE (in %).

Equation:	(6)					(17)					(20)					(19)				
Levels (m)	a	b	R^2	RMSE	UE	a	b	R^2	RMSE	UE	a	b	R^2	RMSE	UE	a	b	R^2	RMSE	UE
Wheat (0.7 m tall)																				
0.7^u	1.07	12.1	0.74	58.3	99	1.05	-0.7	0.79	42.1	87	0.94	15.7	0.66	47.3	99	1.08	-0.8	0.77	45.1	80
1.0^u	1.00	3.5	0.77	45.7	89	1.04	-4.4	0.79	45.5	83	0.92	5.5	0.73	41.7	86	1.08	3.0	0.77	47.5	74
1.3^u	0.99	2.5	0.76	42.4	87	0.97	1.6	0.82	31.0	98	0.90	-2.4	0.78	44.4	81	1.00	-2.0	0.80	34.6	99
All levels ^{u}	1.02	-2.0	0.70	49.4	99	1.04	-11.0	0.79	39.2	99	0.96	-4.5	0.70	44.4	89	1.09	-10.5	0.77	42.5	88
1.3^u *	0.69	-0.5	0.76	89.1	14	0.74	-3.0	0.82	91.6	4	0.67	-1.7	0.78	90.4	8	0.63	-1.3	0.80	114.6	4
Grape Vineyard (2 m tall)																				
2.0^u	1.06	6.5	0.93	29.0	56	1.15	45.2	0.91	80.9	11	0.94	57.4	0.90	52.4	20	0.93	106.2	0.60	108.4	27
2.3^u	1.09	-5.1	0.93	27.0	71	1.11	30.8	0.88	62.6	25	1.01	41.4	0.88	52.7	27	1.00	93.4	0.60	113.2	29
2.6^u	1.02	-4.4	0.94	21.0	98	1.05	27.1	0.91	46.2	31	0.98	39.3	0.90	42.9	31	0.96	92.1	0.61	102.8	32
2.9^u	1.07	-8.4	0.94	20.6	85	1.06	33.0	0.90	53.5	27	1.02	42.2	0.90	53.7	23	0.97	101.9	0.60	114.2	28
All levels ^{u}	1.06	-2.7	0.93	24.7	73	1.09	34.2	0.87	62.2	21	0.99	45.0	0.89	50.6	25	0.97	98.3	0.60	109.7	29
Nectarine orchard (3.2 m tall)																				
3.2^u	-	-	-	-	-	-	-	-	-	-	0.94	-10.2	0.93	18.3	21	0.75	23.5	0.85	25.5	47
$3.2^{u\,1}$	0.93	-10.2	0.91	22.0	23	0.86	20.3	0.71	30.9	87	-	-	-	-	-	-	-	-	-	-
$3.2^{u\,2}$	0.97	16.8	0.93	25.6	45	0.85	31.4	0.85	22.0	62	-	-	-	-	-	-	-	-	-	-
3.2^{2s}	1.00	–13.4	0.30	21.3	60	1.03	-17.6	0.14	28.2	78	-	-	-	-	-	-	-	-	-	-
Olive orchard (3.4 m tall)																				
3.5^u	1.07	13.2	0.93	35.4	62	1.32	8.5	0.89	41.5	27	1.03	10.8	0.85	39.8	82	1.14	8.0	0.85	50.6	79
5.1^u	0.91	5.6	0.93	23.4	91	1.11	4.4	0.90	30.1	48	0.92	3.0	0.87	31.0	86	1.06	1.6	0.88	34.3	88
All levels ^{u}	1.01	3.2	0.94	28.1	89	1.18	4.0	0.90	32.7	41	0.99	3.5	0.87	34.2	97	1.08	3.5	0.87	40.3	82
3.5^s	1.15	1.7	0.98	19.5	13	1.25	-0.5	0.77	12.4	65	-	-	-	-	-	-	-	-	-	-
5.1^s	1.09	0.7	0.83	7.6	99	1.13	0.4	0.78	8.3	77	-	-	-	-	-	-	-	-	-	-
All levels ^{s}	1.11	0.5	0.87	10.6	89	1.19	0.0	0.78	10.3	72	-	-	-	-	-	-	-	-	-	-

Superscripts, s and u denote stable and unstable conditions, respectively.

* Estimates were made assuming the level in the inertial sub-layer.

Friction velocity determined as; (1) $u_* = z/[0.42\,\tau]$ and (2) $u_* = [\langle w'^2 \rangle/1.7]^{0.5}$.

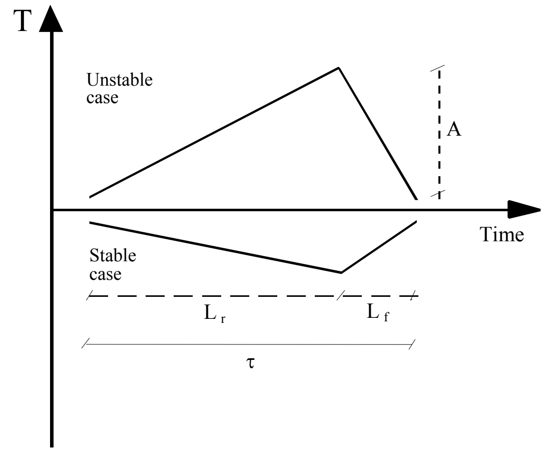

Figure A1

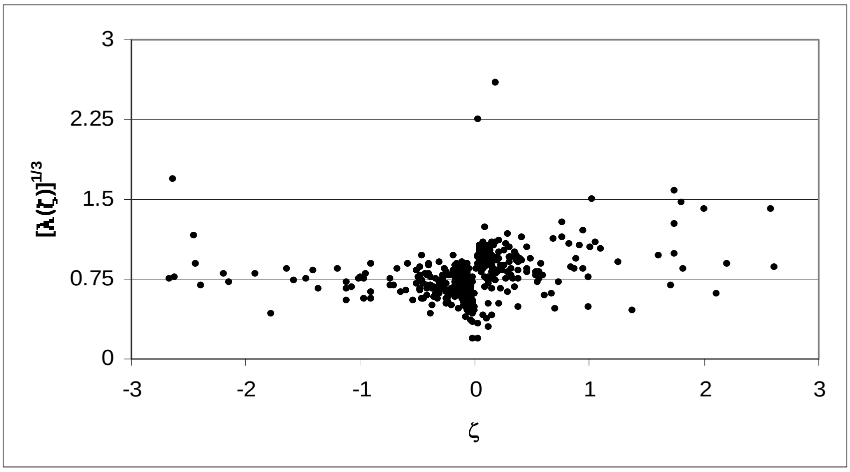

Figure B1a.

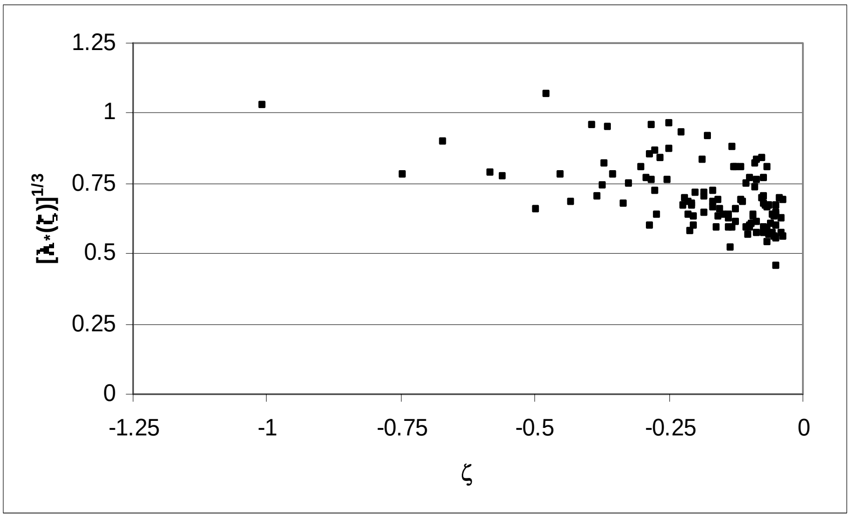

Figure B1b.

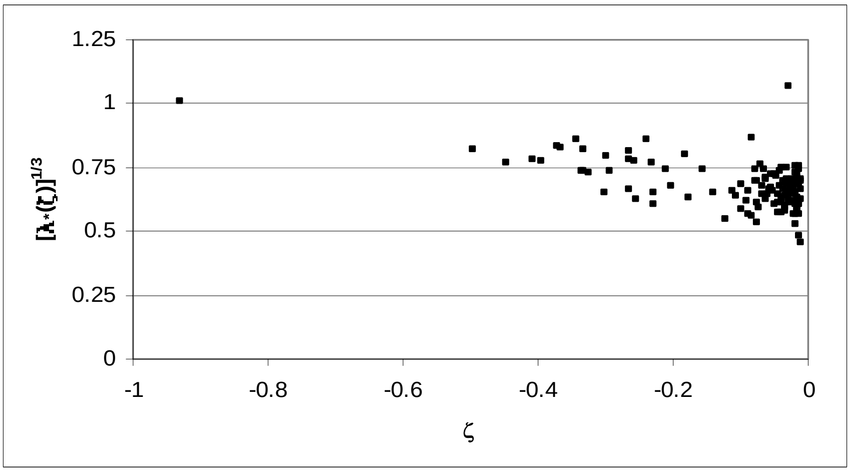

Figure B1c.

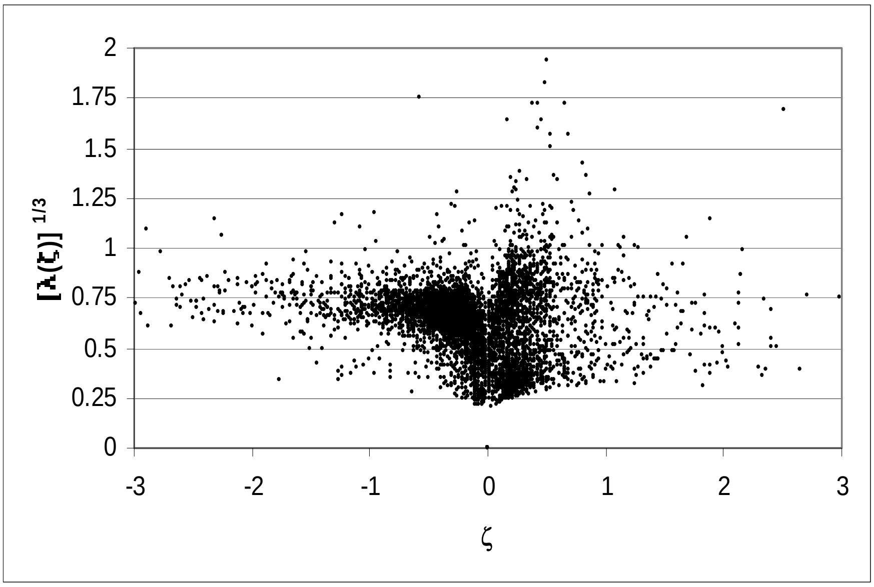

Figure B1d.

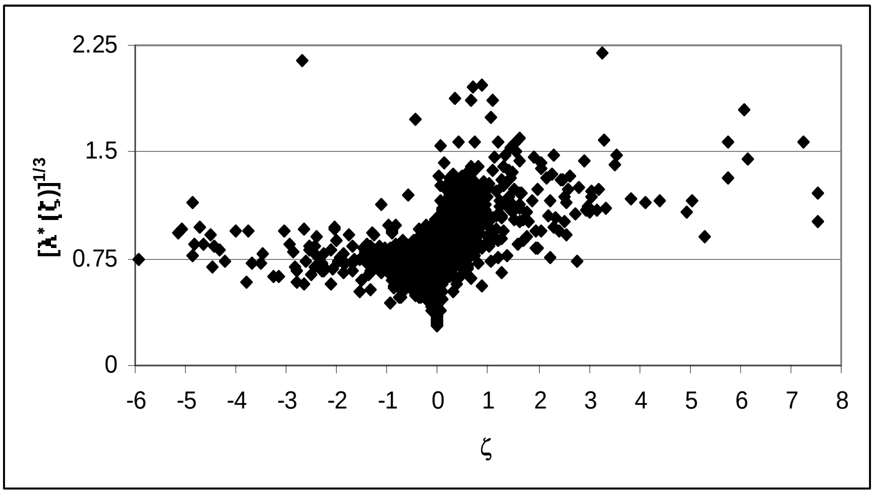

Figure B1e.

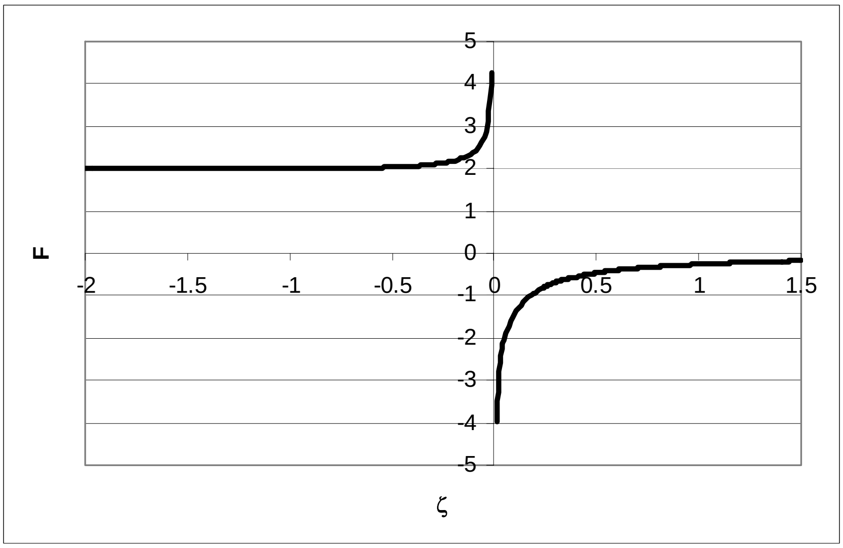

Figure B2.

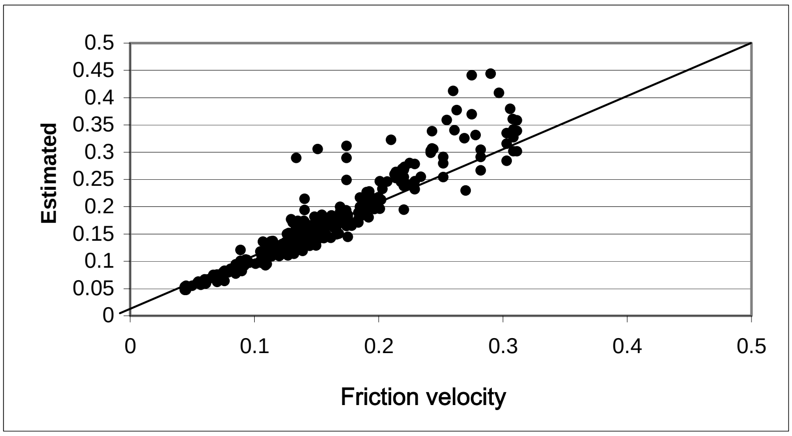

Figure 1a.

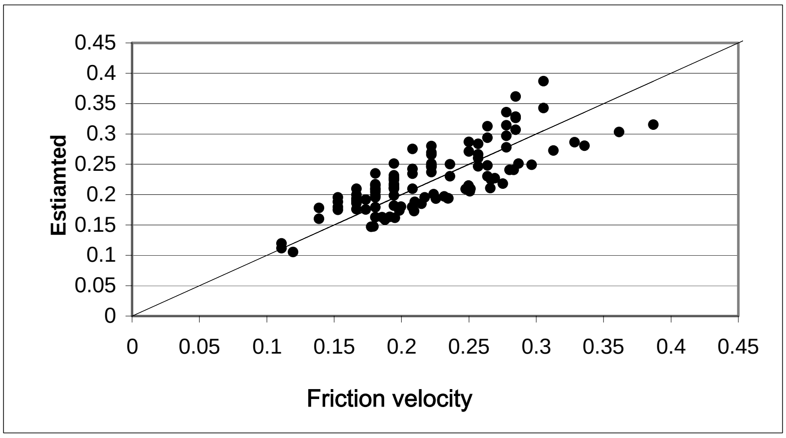

Figure 1b

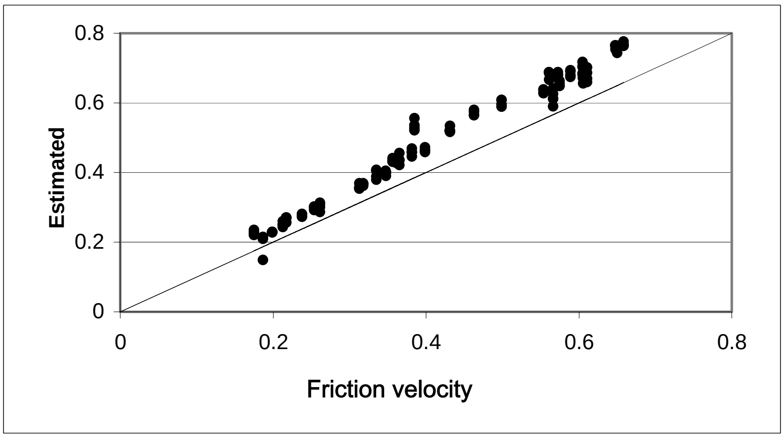

Figure 1c.

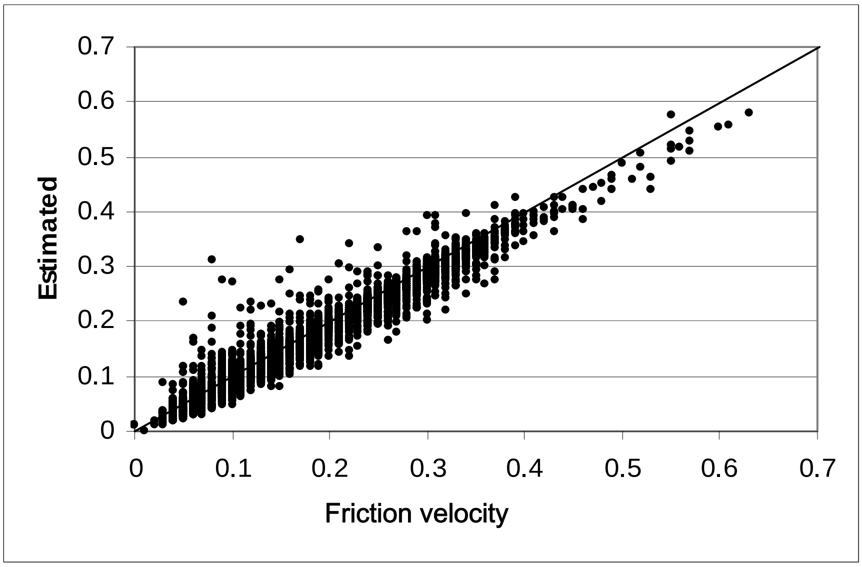

Figure 1d.

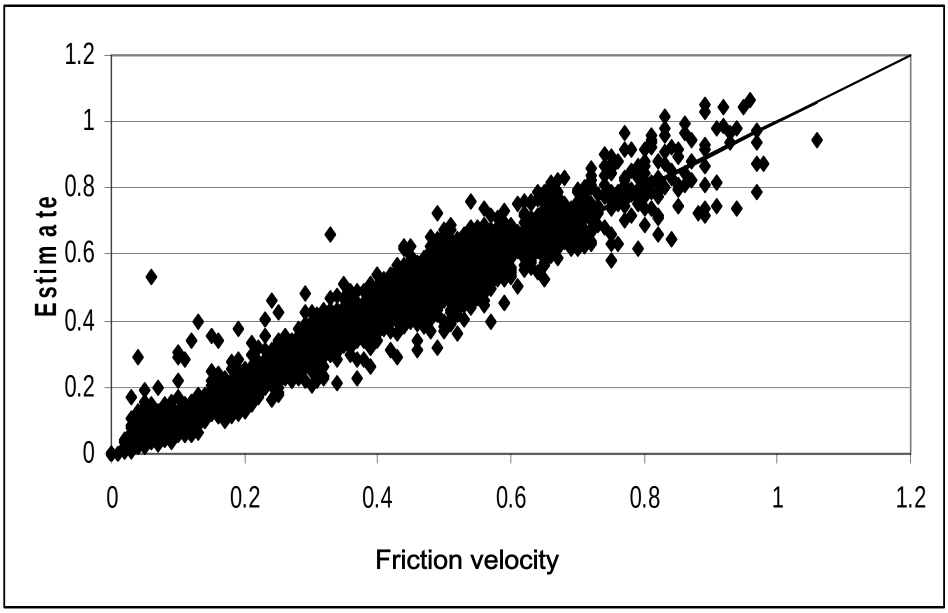

Figure 1e.

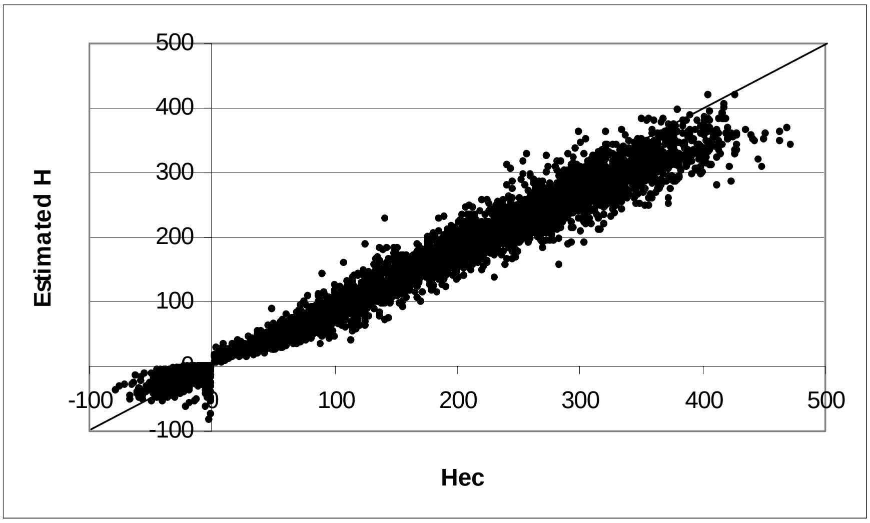

Figure 2a.

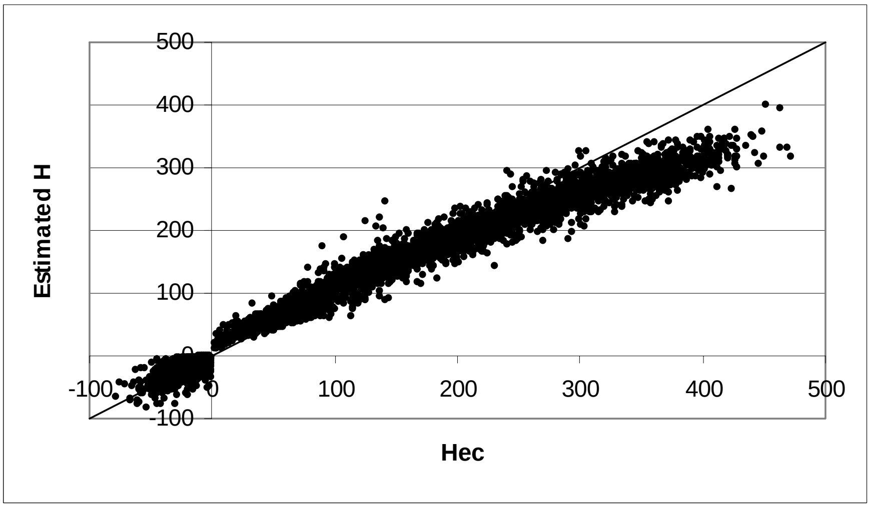

Figure 2b.

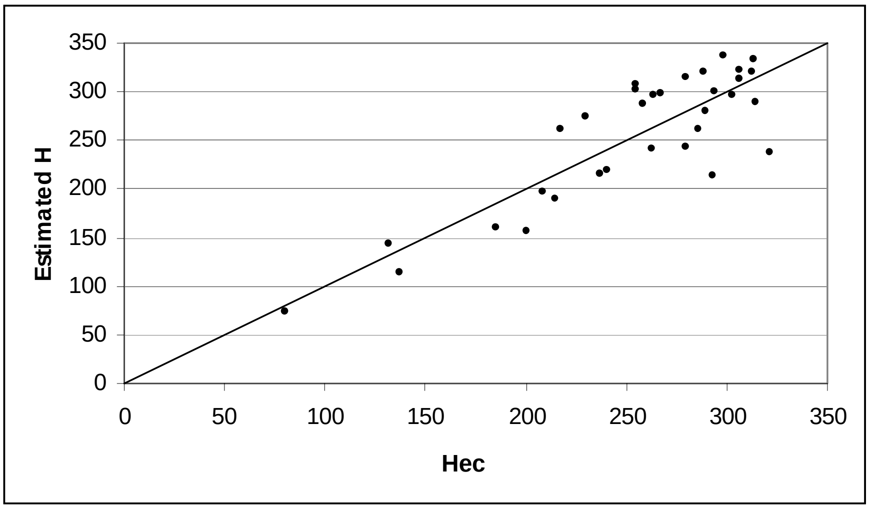

Figure 2c.

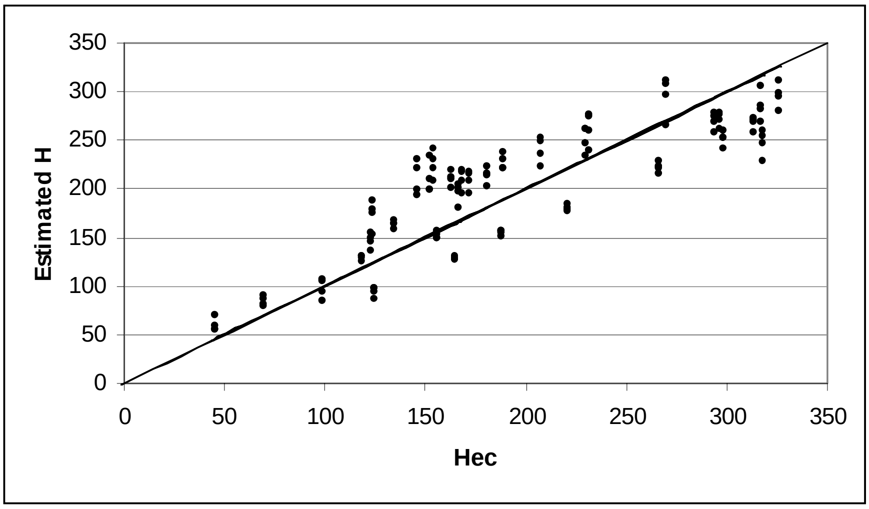

Figure 2d.

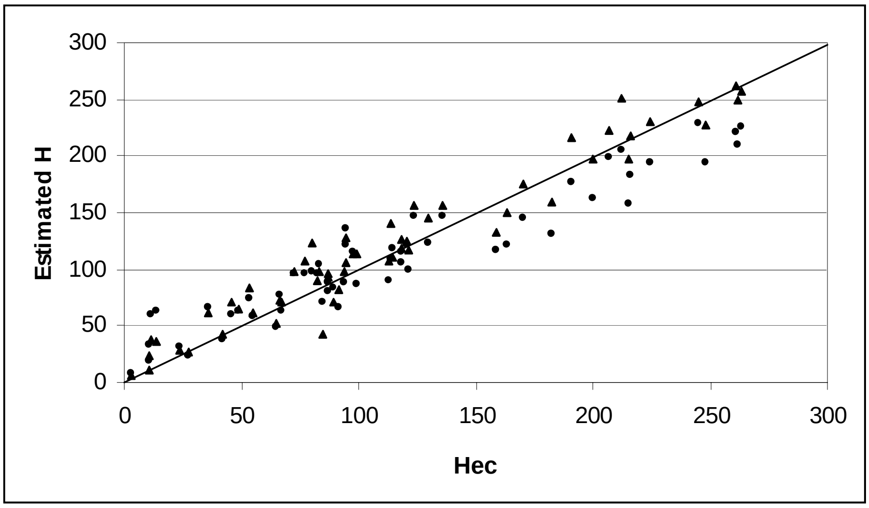

Figure 2e.

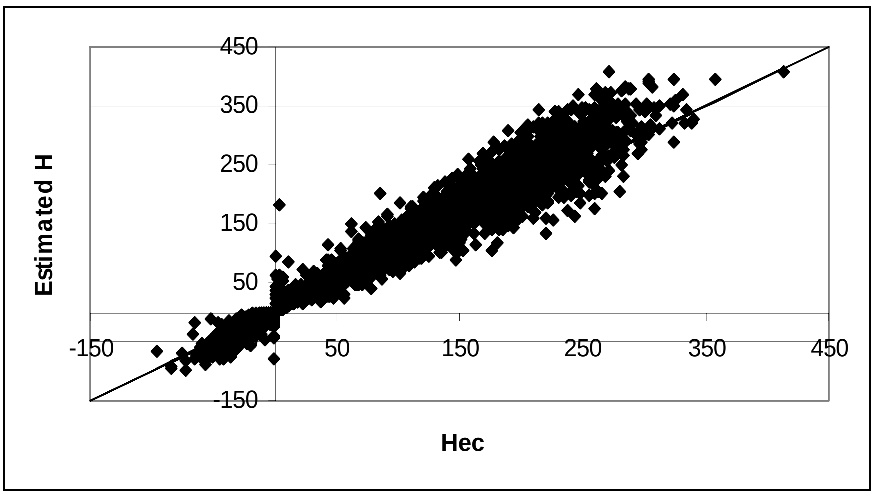

Figure 2f.